Schizophrenia Research 134 (2012) 137–142

Contents lists available at SciVerse ScienceDirect

Schizophrenia Research

journal homepage: www.elsevier.com/locate/schres

Effects of aging on the morphologies of Heschl's gyrus and the superior temporal gyrus in schizophrenia: A postmortem study

Youta Torii [a,*], Shuji Iritani [a,b,c], Hirotaka Sekiguchi [a], Chikako Habuchi [a], Minako Hagikura [a], Tetsuaki Arai [d], Kenji Ikeda [e], Haruhiko Akiyama [c], Norio Ozaki [a]

[a] Department of Psychiatry, Graduate School of Medicine, Nagoya University, 65 Tsurumai, Showa-ku, Nagoya, Aichi 466-8550, Japan
[b] Department of Psychiatry, Tokyo Metropolitan Matsuzawa Hospital, 2-1-1 Kamikitazawa, Setagaya-ku, Tokyo 156-0057, Japan
[c] Department of Psychogeriatrics, Tokyo Institute of Psychiatry, Tokyo Metropolitan Organization for Medical Research, 2-1-8 Kamikitazawa, Setagaya-ku, Tokyo 156-8585, Japan
[d] Department of Psychiatry, Graduate School of Comprehensive Human Sciences, University of Tsukuba, 1-1-1 Tenno-dai, Tsukuba, Ibaraki 305-8575, Japan
[e] Inflammation Pathology, Faculty of Medicine, Kagawa University, 1750-1 Ikenobe, Miki-cho, Kita-gun, Kagawa 761-0793, Japan

ARTICLE INFO

Article history:
Received 16 May 2011
Received in revised form 9 October 2011
Accepted 29 October 2011
Available online 23 November 2011

Keywords:
Schizophrenia
Postmortem study
Aging
Heschl's gyrus
Superior temporal gyrus
Neuropathology

ABSTRACT

The etiology of schizophrenia has been proposed to be neurodevelopmental based on neuroimaging and molecular biological studies. If there is neuronal vulnerability based on neurodevelopment failures in schizophrenic brains, then the impact of aging may have a greater effect on schizophrenic brains than on normal brains. To determine the impact of aging on schizophrenic brains, we investigated the age-related morphological changes of the cross-sectional area of the gray matter (GM) in the left Heschl's gyrus (HG) and the left superior gyrus (STG) in 22 schizophrenic and 24 age- and sex-matched normal control postmortem brains two-dimensionally. The subject groups were divided into younger groups (30–54 years of age) and older groups (65–84 years of age) on the basis of age at death. Both in schizophrenic and control subjects, the GM area in HG and the STG was significantly smaller in the older group than in the younger group, however, no significant differences were observed between the schizophrenic and control subjects. In the STG, the cross-sectional area of the white matter (WM) was also measured. In the older group, the ratio of the GM area to the WM area in the STG was significantly larger in schizophrenic subjects than controls, although there was no significant difference between the schizophrenic and control subjects in the younger group. These findings indicate that the impact of aging has a greater effect on the WM in the STG in schizophrenic subjects than in normal individuals, although the pathological basis is still unclear.

1. Introduction

A decreased cortical volume in schizophrenic brains has been repeatedly reported in cross-sectional imaging studies (Honea et al., 2005; Steen et al., 2006) and postmortem studies (Harrison, 1999; Iritani, 2007). It is understood that this morphological change occurs during the very early period of the formation of the central nervous system, because no gliosis has been found in the postmortem brains of schizophrenic patients (Arnold and Trojanowski, 1996). On the other hand, recent longitudinal imaging studies have also reproducibly reported a greater progressive loss of the cortical volume after disease onset (DeLisi et al., 1997; Kasai et al., 2003b; Nakamura et al., 2007). It is assumed that these phenomena depend on not only neuronal development (Thompson et al., 2001; Vidal et al., 2006) but also continued neuronal degeneration, the long-term use of antipsychotic drugs (Lieberman et al., 2005; Thompson et al., 2009) and unknown interactions between aging and schizophrenia (Harrison, 1999). However, the basis of the volumetric change after disease onset still remains unclear.

To investigate the impact of aging on schizophrenia, it is necessary to consider physiological atrophy and the concomitant presence of neurodegenerative disorders (e.g. Alzheimer-type dementia [ATD], frontotemporal lobar degeneration, etc.) separately. Most neuropathological studies have reported the frequency of Alzheimer-type neuropathological changes in schizophrenic brains to be equal to that in the general population (Powchik et al., 1998; Purohit et al., 1998; Jellinger and Gabriel, 1999), but it remains unclear how the physiological changes in the brain volume of schizophrenic patients occurs, compared to that of the normal brain. To investigate the impact of physiological atrophy, it is necessary to select elderly cases without significant neuropathological changes as study subjects. It is

Abbreviations: ATD, Alzheimer-type dementia; BA, Brodmann area; CPZ, chlorpromazine; CSI, circular sulcus of insula; DTI, diffusion tensor imaging; FTS, first transverse sulcus; GAF, Global Assessment of Functioning; GM, gray matter; HG, Heschl's gyrus; HS, Heschl's sulcus; PMI, postmortem interval; SI, sulcus intermedius; STG, superior temporal gyrus; STS, superior temporal sulcus; WM, white matter.

* Corresponding author. Tel.: +81 52 744 2282; fax: +81 52 744 2293.
E-mail address: youtat@med.nagoya-u.ac.jp (Y. Torii).

0920-9964/$ – see front matter © 2011 Elsevier B.V. All rights reserved.
doi:10.1016/j.schres.2011.10.024

impossible to detect neuropathological changes with the subtle and subclinical concomitant presence of neurodegenerative disorders or other organic factors, such as cerebrovascular changes, by neuroimaging investigations. A postmortem analysis has advantages in that it can determine subtle or subclinical neurodegenerative and organic changes which cannot be detected during the neuroimaging analysis of living subjects. In some cases, early onset frontotemporal dementia, organic psychotic disorders and so on are misdiagnosed as schizophrenia (Fujii et al., 2004; Velakoulis et al., 2009). Generally, schizophrenia is diagnosed based on the operational diagnostic criteria, such as the DSM IV-TR based on clinical symptoms, because so far no definite biological diagnostic tools have yet been established. In addition, neuropathological investigations of the schizophrenic brain are hardly ever performed posthumously in usual clinical settings. Therefore, it is important to perform postmortem neuropathological evaluations, even if the subjects are relatively young at the time of death.

Heschl's gyrus (HG) and its posterior region, the planum temporal (PT), are located on the dorsal surface of the superior temporal gyrus (STG). HG forms part of the primary auditory cortex (Brodmann area [BA] 41/42) and plays a crucial role in auditory perception, while the anterior portion of the PT, which surrounds HG, forms part of the unimodal auditory association cortex (part of BA22) and plays a critical role in language processing (Shapleske et al., 1999). In structural imaging studies, the gray matter (GM) in the STG and its sub-regions, such as HG or the PT, has been found to be smaller (McCarley et al., 2002; Takahashi et al., 2006) and even to decrease over time in schizophrenic patients (Kasai et al., 2003b; Salisbury et al., 2007). Moreover, their reduced size has been correlated with the degree of thought disorder (Shenton et al., 1992; Anderson et al., 2002) and auditory hallucinations (Barta et al., 1990; Onitsuka et al., 2004), especially when the difference is noted on the left side (Sun et al., 2009).

In this study, to determine whether aging has a greater impact on schizophrenic brains than on normal brains, we investigated the age-related changes in the cross-sectional GM area in the left HG and the STG using post-mortem neuropathological slide specimens without significant neuropathological changes. In addition, we also investigated the age-related changes of the cross-sectional area of the white matter (WM) and the ratio of the GM area to the WM area in the left STG to identify differences due to aging in schizophrenic patients and normal subjects.

2. Experimental/Materials and methods

2.1. Subjects

Brain specimens obtained from 22 schizophrenic patients and 24 age- and sex-matched normal control brain specimens were obtained from autopsy cases at Tokyo Metropolitan Matsuzawa Hospital based on the following criterion: age at death ≧30 years and ≦54 years for the younger groups (11 schizophrenic patients, 11 control subjects), and ≧65 years and ≦84 years for the older groups (11 schizophrenic patients, 13 control subjects). The demographic details of the subjects are summarized in Table 1.

We confirmed the diagnosis by reviewing the clinical records to verify that the cases satisfied the DSM-IV-TR criteria for schizophrenia, and that the control subjects had no evidence of psychiatric or neurological disorders.

We also excluded cases with significant neuropathological changes, such as neurodegenerative disorders (e.g. ATD, frontotemporal lobar degeneration, etc.), cerebrovascular diseases, brain invasion of tumors, severe malnutrition, metabolic encephalopathies, inflammatory or traumatic processes, and so on, based on the records of clinico-pathological conferences with several expert neuropathologists. We selected cases without any history of alcohol or substance abuse, convulsions or mental retardation based on the patient clinical records. We confirmed that all cases had sufficient social function before onset and had completed compulsory education.

Table 1
The basic demographic characteristics of the subjects.

	Control		Schizophrenia	
	Younger group	Older group	Younger group	Older group
Number	11	13	11	11
Sex (M/F)	6/5	8/5	7/4	5/6
Age at death (years) range (years)	45.0 ± 8.1 (31–54)	72.7 ± 4.4 (66–81)	44.4 ± 6.8 (33–54)	70.9 ± 5.1 (65–83)
Age at onset (years)	–	–	27.7 ± 13.6	29.7 ± 8.6
Duration of illness (years)	–	–	16.6 ± 10.7	41.2 ± 8.9
Subtype (Paranoid/ Disorganized/Catatonic/ Undifferentiated)	–	–	7/3/1/0	5/4/1/1
GAF scores	–	–	28 ± 4.3	24.3 ± 5.8
Mean daily antipsychotic dosage[d] (mg/day)	–	–	561.3 ± 216.0[a]	562.5 ± 459.6[a]
Lifetime daily antipsychotic dosage[d] (g)	–	–	3343.9 ± 1921.5[a]	8479.4 ± 6139.9[a]
Cause of death (Cardiac/ Respiratory/Other)	3/3/5	2/6/5	1/5/5	1/5/5
Cerebrum weight (kg)	1332.5 ± 165.9[b]	1310.8 ± 206.9	1360.0 ± 171.1	1265.9 ± 149.6
PMI (hours)	6.1 ± 5.4[c]	6.8 ± 4.9[c]	8.3 ± 13.6	10.9 ± 8.6[c]

GAF: Global Assessment of Functioning, PMI: postmortem interval.
There were no significant differences, except for in the age at death and duration of illness, between the younger and older groups ($p<0.01$, Mann–Whitney U test).
[a] Not known for 1 younger subject and 3 older subjects.
[b] Not known for 1 control subject.
[c] Not known for 2 younger control, 2 older control and 2 older schizophrenic subjects.
[d] Chlorpromazine milligram or gram equivalents.

We assessed the clinical severity in the predominant state using the Global Assessment of Functioning (GAF) scale (American Psychiatric Association, 2000), because this scale was easy to pick up retrospectively from the clinical records. It was impossible to evaluate the detailed degrees of symptoms in life retrospectively using the Brief Psychiatric Rating Scale or Positive and Negative Symptom Scale. We measured the sum of antipsychotic dosage taken throughout their lifetime (lifetime antipsychotic dosage) and the mean daily antipsychotic dosage (chlorpromazine [CPZ] milligram equivalents per day) by reviewing the clinical records.

This study was approved by the Nagoya University School of Medicine Ethical Review Board.

2.2. Brain tissue processing

In all cases, the cadavers were kept at 4° C before autopsies to prevent autolysis and tissue degeneration. All brains were extracted and fixed in 10% formalin within 48 h after death. After fixation, the brains were sectioned in the coronal plane. The brains were embedded in paraffin and cut at a thickness of about 10 μm. The sections were stained with hematoxylin-eosin and/or Klüver-Barrera.

2.3. Morphometric analysis

A morphometric analysis was performed by one of the coauthors blind to the diagnosis. In each subject, we used a neuropathological specimen slide from each left coronal slice at the level where HG, the hippocampus and the subthalamic nucleus appeared. Each slice was scanned into a computer as digital data (TIFF file) using an image scanner (CanoScan LiDE 500F; Canon Inc., Japan) at 600 dpi. The tracing and measurements of regions of interest were performed manually using the Adobe Photoshop 6.0 (Adobe Systems Inc., CA,

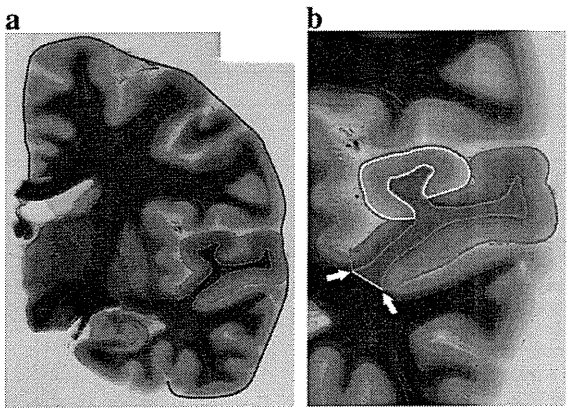

Fig. 1. Delineation of Heschl's gyrus and the superior temporal gyrus. (a) The gray matter (GM) in the left superior temporal gyrus (STG) is shown in red. The length of the external surface of the hemisphere from the callosal sulcus to the occipitotemporal sulcus is shown in blue. (b) The GM in the left STG is shown in red. The GM in the left Heschl's gyrus is shown in yellow. In the STG, after delineating the GM, the boundary of the white matter (WM) was delineated by connecting a straight line between the two open ends of the area of the GM (arrows). The WM in the left STG is shown in green.

USA) and ImageJ 1.43u (free software presented by NIH: http://rsb.info.nih.gov/ij/) software programs on the computer.

We identified the circular sulcus of insula (CSI), Heschl's sulcus (HS), the sulcus intermedius (SI), the first transverse sulcus (FTS) and the superior temporal sulcus (STS). Then, the area of GM bounded by the HS or SI laterally and the FTS medially was delineated and measured as the absolute GM area in HG based on the guidelines for the parcellation of the temporal lobe (Kim et al., 2000) (Fig. 1b). The area of the GM bounded by the STS laterally and the CSI medially was considered the absolute GM area in the STG (Fig. 1a). The length of the external surface of the hemisphere from the callosal sulcus to the occipitotemporal sulcus was measured as the hemisphere circumference (Fig. 1a). The relative GM area in HG and the STG ([absolute GM area of region of interest]/[hemisphere circumference]) was calculated to correct for individual differences in each brain size.

In the STG, after delineating the GM, the boundary of the WM was delineated by connecting a straight line between the two open ends of the area of the GM based on a previous report (Lee et al., 2009). In this way, the absolute WM area was also measured (Fig. 1b). The relative WM area ([absolute WM area of region of interest]/[hemisphere circumference]) and the ratio of the GM area to the WM area was calculated.

2.4. Statistical analysis

For the statistical analyses, nonparametric tests were chosen, because our relatively small sample size was insufficient to evaluate the distribution. The Kruskal–Wallis test was used to assess the differences in the cerebrum weights and postmortem interval (PMI) among the four groups (the younger schizophrenia group, the older schizophrenia group, the younger control group and the older control group). Fisher's exact test was used to assess the differences in gender and causes of death among the four groups, and the differences in subtype between the younger and older schizophrenia groups. The Mann–Whitney *U* test was used to verify the differences in the age at death between the controls and schizophrenic patients in each age group, and the differences in the age at onset, GAF scores or mean daily antipsychotic dosage between the younger and older schizophrenic patients. To assess of impact of aging on the cross-sectional area in regions of interest, the Mann–Whitney *U* test was used between age groups in each diagnostic group and between diagnostic groups in each age group. Spearman's rank correlation was calculated to assess the association between the hemisphere circumference and the cerebrum weight. Spearman's rank correlation was used to assess the association between the cross-sectional area in regions of interest and the PMI, GAF scores or lifetime antipsychotic dosage. The data were expressed as the means ± standard deviation. A value of $p<0.05$ was considered to be statistically significant. All statistical analyses were performed using the SPSS Statistics 17.0 software program (SPSS Inc., IL, USA).

3. Results

The mean values of the cross-sectional area and the hemisphere circumference in each region are reported in Table 2.

3.1. Basic demographic data

There were no significant differences in the gender ($p=0.91$), cause of death ($p=0.90$), cerebrum weight ($p=0.44$) or PMI ($p=0.76$) among the various groups. There were also no significant differences in the age at death between the schizophrenic and control subjects in both the younger and older groups ($p=0.74$, $p=0.26$). There were no significant differences in the age at onset of disease ($p=0.21$), disease subtype ($p=0.82$), GAF scores ($p=0.11$) and mean daily antipsychotic dosage ($p=0.86$) between the younger and older schizophrenic patients.

The PMI and lifetime antipsychotic dosage were not correlated with the cross-sectional area in the regions of interest (the relative GM area in HG; $p=0.53$, $p=0.17$, the relative GM area in the STG; $p=0.67$, $p=0.71$, the relative WM area in the STG; $p=0.51$, $p=0.25$) or the ratio of the GM area to the WM area in the STG ($p=0.91$, $p=0.10$).

3.2. The association between hemisphere circumference and cerebrum weight

The hemisphere circumference was positively correlated with the cerebrum weight in all subjects (Spearman rank correlation, $r=0.44$, $p=0.0034$). As the hemisphere circumference reflected the brain size, it was thought that using the hemisphere circumference was adequate for standardizing individual differences in brain size.

Table 2
The mean values of the cross-sectional area and hemisphere circumference.

	Control		Schizophrenia	
	Younger group	Older group	Younger group	Older group
Hemisphere circumference (mm)	187.2 ± 17.9	178.7 ± 10.2	193.0 ± 12.6	180.2 ± 12.7
HG				
Absolute GM area (mm^2)	58.0 ± 17.0	37.8 ± 17.7	55.6 ± 16.9	39.4 ± 16.6
Relative GM area (mm^2/mm)	0.31 ± 0.10	0.21 ± 0.09	0.29 ± 0.08	0.22 ± 0.10
STG				
Absolute GM area (mm^2)	221.1 ± 46.1	166.9 ± 36.1	212.2 ± 44.6	160.3 ± 31.3
Relative GM area (mm^2/mm)	1.18 ± 0.18	0.93 ± 0.18	1.10 ± 0.21	0.89 ± 0.19
Absolute WM area (mm^2)	84.1 ± 27.4	69.4 ± 22.5	80.7 ± 33.9	54.6 ± 13.4
Relative WM area (mm^2/mm)	0.45 ± 0.12	0.39 ± 0.11	0.42 ± 0.16	0.30 ± 0.07
GM area/WM area (mm^2/mm^2)	2.73 ± 0.49	2.53 ± 0.54	2.82 ± 0.58	3.00 ± 0.48

HG: Heschl's gyrus, STG: superior temporal gyrus, GM: gray matter, WM: white matter.

3.3. The cross-sectional GM area in HG and the STG

The relative GM area in HG was significantly smaller in the older group than in the younger group, in both schizophrenic and control subjects ($p=0.045$, $p=0.02$) (Fig. 2a). However, in both the younger and older groups, there were no significant differences in the relative GM area in HG between the brains from the schizophrenic and control subjects ($p=0.49$, $p=0.58$) (Fig. 2a).

In the STG, the relative GM area was significantly smaller in the older group than in the younger group, in both controls ($p=0.008$) and schizophrenic patients ($p=0.03$) (Fig. 2b). In both the younger and older groups, there were no significant differences in the relative GM area in the STG between the brains of the schizophrenic and control subjects ($p=0.58$, $p=0.58$) (Fig. 2b).

3.4. The cross-sectional WM area in the STG

The relative WM area in the STG was smaller in the older group than the younger group in schizophrenic patients, although this difference was not statistically significant ($p=0.053$), while there was very little age-related reduction in the relative WM area in controls ($p=0.34$) (Fig. 2c). In the younger subjects, there were no significant differences in the relative WM area in the STG between schizophrenic patients and controls ($p=0.49$). In the older groups, the relative WM area in the STG was significantly smaller in the schizophrenic patients than in controls ($p=0.04$) (Fig. 2c). In addition, in the older subjects, the ratio of the GM area to the WM area in the STG was significantly larger in schizophrenic patients than controls ($p=0.04$). However, in the younger groups, there was no significant difference between the ratios in the schizophrenic and control subjects ($p=0.62$) (Fig. 2d).

3.5. The effects of the severity of illness

The GAF scores were positively correlated with the relative GM area in the HG in schizophrenic patients (Spearman's rank correlation, $r=0.48$, $p=0.02$). This correlation was observed especially in the younger schizophrenic patients, although it was barely significant ($r=0.60$, $p=0.050$). On the other hand, in older schizophrenic patients, no correlation was observed ($r=0.10$, $p=0.767$). The GAF scores were not correlated with the relative GM area, WM area or the ratio of the GM area to the WM area in the STG ($p=0.24$, $p=0.23$, $p=0.28$).

4. Discussion

4.1. The GM cross-sectional area and volume reduction in schizophrenic and normal subjects

The first key finding from this study is that there were no significant differences in the cross-sectional GM area loss with age in the STG and its sub-region, HG, between the schizophrenic and normal postmortem brains. We could select elderly subjects without any significant neuropathological changes for the older group, who were older than those in most imaging studies, based on the results of clinico-pathological discussions with several expert neuropathologists and based on physical evidence in the brains themselves observed upon autopsy. It is assumed that the older the subjects are, the stronger the impact of aging would be, however, even the older age of our current subjects did not show any significant impact on the acceleration of GM area reduction, or physiological atrophy, in the schizophrenic brains. Longitudinal imaging studies of the STG and HG have demonstrated the progressive reduction of the GM volume to be larger in the early stage of illness (Jacobsen et al., 1998; Kasai et al., 2003a, 2003b; Salisbury et al., 2007), while the GM volume thereafter stabilizes during the chronic stage of illness (DeLisi and Hoff, 2005; Yoshida et al., 2009). Taking these findings from longitudinal imaging studies into consideration, our results support the assumption that the progression of the GM volume reduction in the STG and its sub-regions in schizophrenic patients does not reflect a greater impact of aging on schizophrenic brains, but such progression is instead due to the neurodevelopmental or neurodegenerative pathogenetic core at the initial stage of schizophrenia.

In our study, no significant differences were seen in the GM area between the schizophrenic and control subjects in the younger groups. A few imaging studies reported results consistent with our findings (Kulynych et al., 1996; Barta et al., 1997). Nevertheless, GM or total volume reduction in the STG in patients with schizophrenia

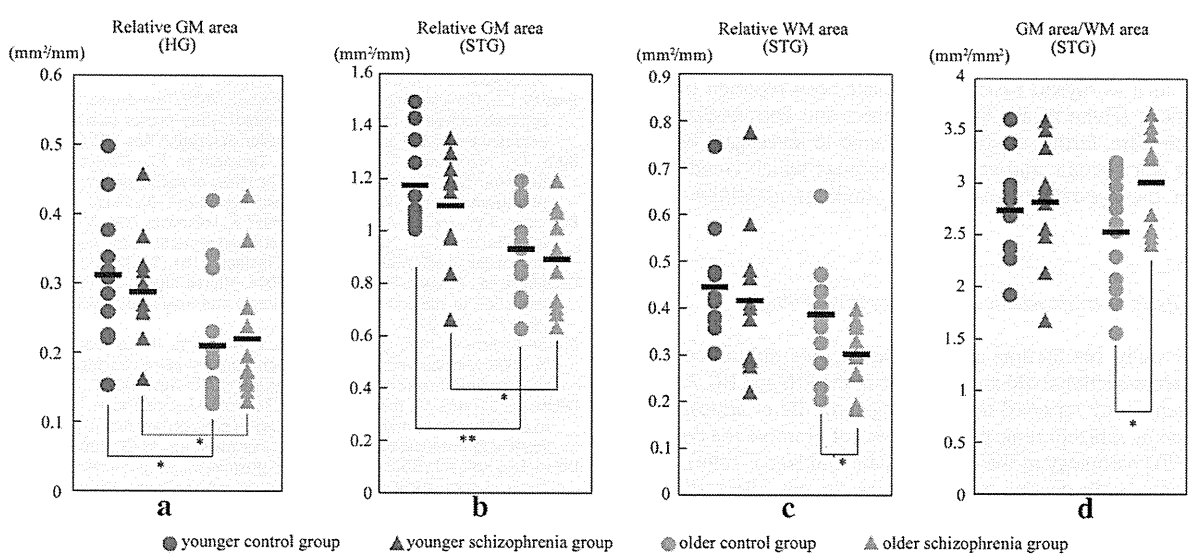

Fig. 2. Effects of aging on Heschl's gyrus and the superior temporal gyrus in the schizophrenic and control subjects. (a) The relative gray matter (GM) area in Heschl's gyrus (HG) in the schizophrenic and control subjects. (b) The relative GM area in the superior temporal gyrus (STG) in the subjects with schizophrenia and the controls. (c) The relative white matter (WM) area in the STG in the schizophrenic and control subjects. (d) The ratio of the GM area to the WM area in the STG in the subjects with schizophrenia and the controls. The horizontal black lines indicate the means. **: $p<0.01$, *: $p<0.05$.

has also been frequently reported in some imaging studies where the mean age is in the 40s, which is equal to that of our younger group (Anderson et al., 2002; Onitsuka et al., 2004). In comparison to the findings of imaging studies, this discrepancy may be explained by the older mean age at onset and the shorter illness duration of our younger group (Matsumoto et al., 2001; Crespo-Facorro et al., 2004; DeLisi and Hoff, 2005), in addition to the methodological differences.

4.2. WM cross-sectional area or volume reduction in schizophrenia

Our second key finding is that the WM loss increased with age in the STG in the schizophrenic patients, but not in the controls. In younger schizophrenic patients, some cross-sectional imaging studies have reported an absence of volumetric differences in the WM in the STG (Gur et al., 2000; Matsumoto et al., 2001; Buchanan et al., 2004), which is in agreement with our finding, although other studies have reported volumetric differences (Spalletta et al., 2003; O'Daly et al., 2007). To the best of our knowledge, there have been no previous reports about volumetric changes in the WM in the STG in elderly schizophrenic patients. With regard to other brain regions, there have been a few reports about volumetric changes of the WM with age. Our finding is in agreement with the studies which have noted an increase in the WM loss with age in schizophrenic patients in the frontal lobes (Ho et al., 2003) and total brain (Bose et al., 2009) and is in contrast to a study that reported no difference in the WM loss with age in the total brain between schizophrenic and control subjects (Hulshoff Pol et al., 2002). Therefore, controversy remains in regard to whether there is a WM volume change as a result of schizophrenia.

Recent diffusion tensor imaging (DTI) studies have repeatedly reported WM abnormalities in schizophrenic patients based on decreases in anisotropy indices in the WM tracts and structures (Hubl et al., 2004; Wang et al., 2004). It is thought that the WM changes noted in DTI studies could reflect a loss of organization in WM fiber tracts, such as loss of myelin, axonal fibers, and/or increased extracellular space in this region. However, further examinations will be required to determine what volumetric change in the WM is reflected in our studies, because there were differences in the methodologies between the various studies.

In postmortem studies, in addition to reduced glial cell density (Beasley et al., 2009) in the WM in the STG in schizophrenic patients, it has been demonstrated that there is decreased expression of myelination-related genes (e.g. CNP, MAG, PLP1, ERBB3, etc.) (Tkachev et al., 2003; Peirce et al., 2006) and decreased intracortical myelin markers, such as myelin basic protein, have been reported in other brain regions (Flynn et al., 2003; Chambers and Perrone-Bizzozero, 2004). Therefore, further studies are required to investigate whether there are microscopic and/or genetic findings which could correlate with the age-related macroscopic findings identified in our studies.

4.3. The effects of antipsychotics and the severity of illness

In our study, the lifetime antipsychotic dosage did not correlate with the cross-sectional GM and WM area in the STG and HG. Another postmortem study reported that the long-term use of antipsychotic medication by schizophrenic patients does not promote the development of ATD pathology in the brain (Niizato and Ikeda, 1996). These findings may indicate that antipsychotics do not affect the age-related changes of the brain tissue.

In our study, the severity of illness was more likely to affect the brain volume in the younger patients, not in older patients. This finding may be due to many factors related to aging, such as physical disease. It is assumed that the effects of schizophrenia itself may be obscured by many of these factors.

4.4. Future studies

There are a few limitations to this study. First, we measured the morphological changes two-dimensionally in glass slide specimens. It would therefore be better to measure the actual volume of HG and the STG three-dimensionally, but it is difficult to measure the volume when evaluating two-dimensional glass slide specimens. Second, our data cannot be directly compared with the data of neuroimaging studies, because the brain tissue would likely constrict during the course of fixation.

Ultimately, a histopathological or neuropathological investigation of the WM of schizophrenic patients, focusing on the formation of the neuronal fibers, including neurofilament or myelin protein, is thus called for to elucidate the pathological basis of our age-related findings.

Role of funding source

This research was supported by Grants-in-Aid for Scientific Research (No. 20591400) from the Japan Society for the Promotion of Science (2008–2010).

Contributors

The study was conceptualized by SI, TA and KI. The sample was controlled by YT, SI, TA, KI and HA. The analyses were designed and conducted by YT, HS, CH and NO. The manuscript was written by YT, SI, HS, CH, MH and NO. All authors have approved the final manuscript.

Conflict of interest

None.

Acknowledgments

None.

References

American Psychiatric Association, 2000. Diagnostic and Statistical Manual of Mental Disorders, 4th Edition, Text Revision (DSM-IV-TR). American Psychiatric Association, Washington DC.

Anderson, J.E., Wible, C.G., McCarley, R.W., Jakab, M., Kasai, K., Shenton, M.E., 2002. An MRI study of temporal lobe abnormalities and negative symptoms in chronic schizophrenia. Schizophr. Res. 58 (2–3), 123–134.

Arnold, S.E., Trojanowski, J.Q., 1996. Recent advances in defining the neuropathology of schizophrenia. Acta Neuropathol 92 (3), 217–231.

Barta, P.E., Pearlson, G.D., Powers, R.E., Richards, S.S., Tune, L.E., 1990. Auditory hallucinations and smaller superior temporal gyral volume in schizophrenia. Am. J. Psychiatry 147 (11), 1457–1462.

Barta, P.E., Pearlson, G.D., Brill 2nd, L.B., Royall, R., McGilchrist, I.K., Pulver, A.E., Powers, R.E., Casanova, M.F., Tien, A.Y., Frangou, S., Petty, R.G., 1997. Planum temporale asymmetry reversal in schizophrenia: replication and relationship to gray matter abnormalities. Am. J. Psychiatry 154 (5), 661–667.

Beasley, C.L., Honavar, M., Everall, I.P., Cotter, D., 2009. Two-dimensional assessment of cytoarchitecture in the superior temporal white matter in schizophrenia, major depressive disorder and bipolar disorder. Schizophr. Res. 115 (2–3), 156–162.

Bose, S.K., Mackinnon, T., Mehta, M.A., Turkheimer, F.E., Howes, O.D., Selvaraj, S., Kempton, M.J., Grasby, P.M., 2009. The effect of ageing on grey and white matter reductions in schizophrenia. Schizophr. Res. 112 (1–3), 7–13.

Buchanan, R.W., Francis, A., Arango, C., Miller, K., Lefkowitz, D.M., McMahon, R.P., Barta, P.E., Pearlson, G.D., 2004. Morphometric assessment of the heteromodal association cortex in schizophrenia. Am. J. Psychiatry 161 (2), 322–331.

Chambers, J.S., Perrone-Bizzozero, N.I., 2004. Altered myelination of the hippocampal formation in subjects with schizophrenia and bipolar disorder. Neurochem. Res. 29 (12), 2293–2302.

Crespo-Facorro, B., Kim, J.J., Chemerinski, E., Magnotta, V., Andreasen, N.C., Nopoulos, P., 2004. Morphometry of the superior temporal plane in schizophrenia: relationship to clinical correlates. J Neuropsychiatry Clin Neurosci 16 (3), 284–294.

DeLisi, L.E., Sakuma, M., Tew, W., Kushner, M., Hoff, A.L., Grimson, R., 1997. Schizophrenia as a chronic active brain process: a study of progressive brain structural change subsequent to the onset of schizophrenia. Psychiatry Res 74 (3), 129–140.

DeLisi, L.E., Hoff, A.L., 2005. Failure to find progressive temporal lobe volume decreases 10 years subsequent to a first episode of schizophrenia. Psychiatry Res 138 (3), 265–268.

Flynn, S.W., Lang, D.J., Mackay, A.L., Goghari, V., Vavasour, I.M., Whittall, K.P., Smith, G. N., Arango, V., Mann, J.J., Dwork, A.J., Falkai, P., Honer, W.G., 2003. Abnormalities of myelination in schizophrenia detected in vivo with MRI, and post-mortem with analysis of oligodendrocyte proteins. Mol Psychiatry 8 (9), 811–820.

Fujii, D., Ahmed, I., Hishinuma, E., 2004. A neuropsychological comparison of psychotic disorder following traumatic brain injury, traumatic brain injury without psychotic disorder, and schizophrenia. J Neuropsychiatry Clin Neurosci 16 (3), 306–314.

Gur, R.E., Turetsky, B.I., Cowell, P.E., Finkelman, C., Maany, V., Grossman, R.I., Arnold, S. E., Bilker, W.B., Gur, R.C., 2000. Temporolimbic volume reductions in schizophrenia. Arch. Gen. Psychiatry 57 (8), 769–775.
Harrison, P.J., 1999. The neuropathology of schizophrenia. A critical review of the data and their interpretation. Brain 122 (Pt 4), 593–624.
Ho, B.C., Andreasen, N.C., Nopoulos, P., Arndt, S., Magnotta, V., Flaum, M., 2003. Progressive structural brain abnormalities and their relationship to clinical outcome: a longitudinal magnetic resonance imaging study early in schizophrenia. Arch. Gen. Psychiatry 60 (6), 585–594.
Honea, R., Crow, T.J., Passingham, D., Mackay, C.E., 2005. Regional deficits in brain volume in schizophrenia: a meta-analysis of voxel-based morphometry studies. Am. J. Psychiatry 162 (12), 2233–2245.
Hubl, D., Koenig, T., Strik, W., Federspiel, A., Kreis, R., Boesch, C., Maier, S.E., Schroth, G., Lovblad, K., Dierks, T., 2004. Pathways that make voices: white matter changes in auditory hallucinations. Arch. Gen. Psychiatry 61 (7), 658–668.
Hulshoff Pol, H.E., Schnack, H.G., Bertens, M.G., van Haren, N.E., van der Tweel, I., Staal, W.G., Baare, W.F., Kahn, R.S., 2002. Volume changes in gray matter in patients with schizophrenia. Am. J. Psychiatry 159 (2), 244–250.
Iritani, S., 2007. Neuropathology of schizophrenia: a mini review. Neuropathology 27 (6), 604–608.
Jacobsen, L.K., Giedd, J.N., Castellanos, F.X., Vaituzis, A.C., Hamburger, S.D., Kumra, S., Lenane, M.C., Rapoport, J.L., 1998. Progressive reduction of temporal lobe structures in childhood-onset schizophrenia. Am. J. Psychiatry 155 (5), 678–685.
Jellinger, K.A., Gabriel, E., 1999. No increased incidence of Alzheimer's disease in elderly schizophrenics. Acta Neuropathol 97 (2), 165–169.
Kasai, K., Shenton, M.E., Salisbury, D.F., Hirayasu, Y., Lee, C.U., Ciszewski, A.A., Yurgelun-Todd, D., Kikinis, R., Jolesz, F.A., McCarley, R.W., 2003a. Progressive decrease of left superior temporal gyrus gray matter volume in patients with first-episode schizophrenia. Am. J. Psychiatry 160 (1), 156–164.
Kasai, K., Shenton, M.E., Salisbury, D.F., Hirayasu, Y., Onitsuka, T., Spencer, M.H., Yurgelun-Todd, D.A., Kikinis, R., Jolesz, F.A., McCarley, R.W., 2003b. Progressive decrease of left Heschl gyrus and planum temporale gray matter volume in first-episode schizophrenia: a longitudinal magnetic resonance imaging study. Arch. Gen. Psychiatry 60 (8), 766–775.
Kim, J.J., Crespo-Facorro, B., Andreasen, N.C., O'Leary, D.S., Zhang, B., Harris, G., Magnotta, V.A., 2000. An MRI-based parcellation method for the temporal lobe. NeuroImage 11 (4), 271–288.
Kulynych, J.J., Vladar, K., Jones, D.W., Weinberger, D.R., 1996. Superior temporal gyrus volume in schizophrenia: a study using MRI morphometry assisted by surface rendering. Am. J. Psychiatry 153 (1), 50–56.
Lee, K., Yoshida, T., Kubicki, M., Bouix, S., Westin, C.F., Kindlmann, G., Niznikiewicz, M., Cohen, A., McCarley, R.W., Shenton, M.E., 2009. Increased diffusivity in superior temporal gyrus in patients with schizophrenia: a Diffusion Tensor Imaging study. Schizophr. Res. 108 (1–3), 33–40.
Lieberman, J.A., Tollefson, G.D., Charles, C., Zipursky, R., Sharma, T., Kahn, R.S., Keefe, R. S., Green, A.I., Gur, R.E., McEvoy, J., Perkins, D., Hamer, R.M., Gu, H., Tohen, M., 2005. Antipsychotic drug effects on brain morphology in first-episode psychosis. Arch. Gen. Psychiatry 62 (4), 361–370.
Matsumoto, H., Simmons, A., Williams, S., Hadjulis, M., Pipe, R., Murray, R., Frangou, S., 2001. Superior temporal gyrus abnormalities in early-onset schizophrenia: similarities and differences with adult-onset schizophrenia. Am. J. Psychiatry 158 (8), 1299–1304.
McCarley, R.W., Salisbury, D.F., Hirayasu, Y., Yurgelun-Todd, D.A., Tohen, M., Zarate, C., Kikinis, R., Jolesz, F.A., Shenton, M.E., 2002. Association between smaller left posterior superior temporal gyrus volume on magnetic resonance imaging and smaller left temporal P300 amplitude in first-episode schizophrenia. Arch. Gen. Psychiatry 59 (4), 321–331.
Nakamura, M., Salisbury, D.F., Hirayasu, Y., Bouix, S., Pohl, K.M., Yoshida, T., Koo, M.S., Shenton, M.E., McCarley, R.W., 2007. Neocortical gray matter volume in first-episode schizophrenia and first-episode affective psychosis: a cross-sectional and longitudinal MRI study. Biol. Psychiatry 62 (7), 773–783.
Niizato, K., Ikeda, K., 1996. Long-term antipsychotic medication of schizophrenics does not promote the development of Alzheimer's disease brain pathology. J. Neurol. Sci. 138 (1–2), 165–167.
O'Daly, O.G., Frangou, S., Chitnis, X., Shergill, S.S., 2007. Brain structural changes in schizophrenia patients with persistent hallucinations. Psychiatry Res 156 (1), 15–21.
Onitsuka, T., Shenton, M.E., Salisbury, D.F., Dickey, C.C., Kasai, K., Toner, S.K., Frumin, M., Kikinis, R., Jolesz, F.A., McCarley, R.W., 2004. Middle and inferior temporal gyrus gray matter volume abnormalities in chronic schizophrenia: an MRI study. Am. J. Psychiatry 161 (9), 1603–1611.
Peirce, T.R., Bray, N.J., Williams, N.M., Norton, N., Moskvina, V., Preece, A., Haroutunian, V., Buxbaum, J.D., Owen, M.J., O'Donovan, M.C., 2006. Convergent evidence for 2′,3′-cyclic nucleotide 3′-phosphodiesterase as a possible susceptibility gene for schizophrenia. Arch. Gen. Psychiatry 63 (1), 18–24.
Powchik, P., Davidson, M., Haroutunian, V., Gabriel, S.M., Purohit, D.P., Perl, D.P., Harvey, P.D., Davis, K.L., 1998. Postmortem studies in schizophrenia. Schizophr. Bull. 24 (3), 325–341.
Purohit, D.P., Perl, D.P., Haroutunian, V., Powchik, P., Davidson, M., Davis, K.L., 1998. Alzheimer disease and related neurodegenerative diseases in elderly patients with schizophrenia: a postmortem neuropathologic study of 100 cases. Arch. Gen. Psychiatry 55 (3), 205–211.
Salisbury, D.F., Kuroki, N., Kasai, K., Shenton, M.E., McCarley, R.W., 2007. Progressive and interrelated functional and structural evidence of post-onset brain reduction in schizophrenia. Arch. Gen. Psychiatry 64 (5), 521–529.
Shapleske, J., Rossell, S.L., Woodruff, P.W., David, A.S., 1999. The planum temporale: a systematic, quantitative review of its structural, functional and clinical significance. Brain Res Brain Res Rev 29 (1), 26–49.
Shenton, M.E., Kikinis, R., Jolesz, F.A., Pollak, S.D., LeMay, M., Wible, C.G., Hokama, H., Martin, J., Metcalf, D., Coleman, M., et al., 1992. Abnormalities of the left temporal lobe and thought disorder in schizophrenia. A quantitative magnetic resonance imaging study. N. Engl. J. Med. 327 (9), 604–612.
Spalletta, G., Tomaiuolo, F., Marino, V., Bonaviri, G., Trequattrini, A., Caltagirone, C., 2003. Chronic schizophrenia as a brain misconnection syndrome: a white matter voxel-based morphometry study. Schizophr. Res. 64 (1), 15–23.
Steen, R.G., Mull, C., McClure, R., Hamer, R.M., Lieberman, J.A., 2006. Brain volume in first-episode schizophrenia: systematic review and meta-analysis of magnetic resonance imaging studies. Br. J. Psychiatry 188, 510–518.
Sun, J., Maller, J.J., Guo, L., Fitzgerald, P.B., 2009. Superior temporal gyrus volume change in schizophrenia: a review on region of interest volumetric studies. Brain Res. Rev. 61 (1), 14–32.
Takahashi, T., Suzuki, M., Zhou, S.Y., Tanino, R., Hagino, H., Kawasaki, Y., Matsui, M., Seto, H., Kurachi, M., 2006. Morphologic alterations of the parcellated superior temporal gyrus in schizophrenia spectrum. Schizophr. Res. 83 (2–3), 131–143.
Thompson, P.M., Vidal, C., Giedd, J.N., Gochman, P., Blumenthal, J., Nicolson, R., Toga, A. W., Rapoport, J.L., 2001. Mapping adolescent brain change reveals dynamic wave of accelerated gray matter loss in very early-onset schizophrenia. Proc. Natl. Acad. Sci. U. S. A. 98 (20), 11650–11655.
Thompson, P.M., Bartzokis, G., Hayashi, K.M., Klunder, A.D., Lu, P.H., Edwards, N., Hong, M.S., Yu, M., Geaga, J.A., Toga, A.W., Charles, C., Perkins, D.O., McEvoy, J., Hamer, R. M., Tohen, M., Tollefson, G.D., Lieberman, J.A., 2009. Time-lapse mapping of cortical changes in schizophrenia with different treatments. Cereb Cortex 19 (5), 1107–1123.
Tkachev, D., Mimmack, M.L., Ryan, M.M., Wayland, M., Freeman, T., Jones, P.B., Starkey, M., Webster, M.J., Yolken, R.H., Bahn, S., 2003. Oligodendrocyte dysfunction in schizophrenia and bipolar disorder. Lancet 362 (9386), 798–805.
Velakoulis, D., Walterfang, M., Mocellin, R., Pantelis, C., McLean, C., 2009. Frontotemporal dementia presenting as schizophrenia-like psychosis in young people: clinicopathological series and review of cases. Br. J. Psychiatry 194 (4), 298–305.
Vidal, C.N., Rapoport, J.L., Hayashi, K.M., Geaga, J.A., Sui, Y., McLemore, L.E., Alaghband, Y., Giedd, J.N., Gochman, P., Blumenthal, J., Gogtay, N., Nicolson, R., Toga, A.W., Thompson, P.M., 2006. Dynamically spreading frontal and cingulate deficits mapped in adolescents with schizophrenia. Arch. Gen. Psychiatry 63 (1), 25–34.
Wang, F., Sun, Z., Cui, L., Du, X., Wang, X., Zhang, H., Cong, Z., Hong, N., Zhang, D., 2004. Anterior cingulum abnormalities in male patients with schizophrenia determined through diffusion tensor imaging. Am. J. Psychiatry 161 (3), 573–575.
Yoshida, T., McCarley, R.W., Nakamura, M., Lee, K., Koo, M.S., Bouix, S., Salisbury, D.F., Morra, L., Shenton, M.E., Niznikiewicz, M.A., 2009. A prospective longitudinal volumetric MRI study of superior temporal gyrus gray matter and amygdala-hippocampal complex in chronic schizophrenia. Schizophr. Res. 113 (1), 84–94.

Molecular Psychiatry (2011) 16, 307–320

www.nature.com/mp

ORIGINAL ARTICLE

Transient exposure of neonatal mice to neuregulin-1 results in hyperdopaminergic states in adulthood: implication in neurodevelopmental hypothesis for schizophrenia

T Kato[1], Y Abe[1], H Sotoyama[1], A Kakita[2], R Kominami[3], S Hirokawa[3], M Ozaki[4], H Takahashi[2], and H Nawa[1]

[1]*Department of Molecular Neurobiology, Brain Research Institute, Niigata University, Niigata, Japan;* [2]*Department of Pathological Neuroscience, Resource Branch for Brain Disease Research, Brain Research Institute, Niigata University, Niigata, Japan;* [3]*Department of Molecular Genetics, Niigata University, Niigata, Japan and* [4]*Consolidated Research Institute for Advanced Science and Medical Care, Waseda University, Tokyo, Japan*

Neuregulin-1 (NRG1) is implicated in the etiology or pathology of schizophrenia, although its biological roles in this illness are not fully understood. Human midbrain dopaminergic neurons highly express NRG1 receptors (ErbB4). To test its neuropathological role in the neurodevelopmental hypothesis of schizophrenia, we administered type-1 NRG1 protein to neonatal mice and evaluated the immediate and subsequent effects on dopaminergic neurons and their associated behaviors. Peripheral NRG1 administration activated midbrain ErbB4 and elevated the expression, phosphorylation and enzyme activity of tyrosine hydroxylase (TH), which ultimately increased dopamine levels. The hyperdopaminergic state was sustained in the medial prefrontal cortex after puberty. There were marked increases in dopaminergic terminals and TH levels. In agreement, higher amounts of dopamine were released from this brain region of NRG1-treated mice following high potassium stimulation. Furthermore, NRG1-treated mice exhibited behavioral impairments in prepulse inhibition, latent inhibition, social behaviors and hypersensitivity to methamphetamine. However, there were no gross abnormalities in brain structures or other phenotypic features of neurons and glial cells. Collectively, our findings provide novel insights into neurotrophic contribution of NRG1 to dopaminergic maldevelopment and schizophrenia pathogenesis.
Molecular Psychiatry (2011) **16,** 307–320; doi:10.1038/mp.2010.10; published online 9 February 2010

Keywords: NRG1; dopamine; schizophrenia; ErbB4; TH; neurotrophic factor

Introduction

Neurodevelopmental deficits are considered to be the key features of schizophrenia, which is a multifactorial disease involving environmental factors/insults and genetic predispositions, such as a genetic polymorphism of the neurotrophic factor *neuregulin-1* (*NRG1*). *NRG1* and its receptor (*ErbB4*) were identified as susceptibility genes for schizophrenia.[1,2] Changes in the expression levels of NRG1 splicing isoforms and ErbB4 protein are also found in postmortem brains and peripheral blood cells of schizophrenia patients,[3–6] although the pathophysiological contribution of abnormal NRG1/ErbB4 signaling to schizophrenia is largely unresolved. In this neurodevelopmental hypothesis of schizophrenia, the environmental factors include maternal infection, abnormal delivery and neonatal hypoxia, which presumably interact with the risk genes of schizophrenia.[7,8] For example, schizophrenia-related single-nucleotide polymorphisms (SNPs) of the *NRG1* gene are often located in its promoter regions and positively regulate gene transcription.[1,5] NRG1 expression is induced by adult ischemic and traumatic brain injury, as well as by neonatal hypoxia.[9–11] Thus, it is possible that the more abnormal expression of NRG1 is induced in human embryos or neonates carrying these SNPs by these environmental insults, the more severely this factor might impair brain development to increase the risk of schizophrenia.

Neuregulin-1 is one of the neurodevelopmental regulators that are involved in neuronal migration, axon pathway finding, myelination and synaptogenesis.[12–15] Thus, the abnormality in its expression can be implicated in the neurodevelopmental hypothesis mentioned above. Accordingly, various exons of the

Correspondence: Dr H Nawa, Department of Molecular Neurobiology, Brain Research Institute, Niigata University, 1–757 Asahimachi-dori, Niigata, 951–8585, Japan.
E-mail: hnawa@bri.niigata-u.ac.jp
Received 7 November 2009; revised 22 December 2009; accepted 13 January 2010; published online 9 February 2010

NRG1 genome have been disrupted by homologous recombination in mice and their neurobehavioral traits have been investigated.[1,16–19] In adults, the mutant mice of NRG1 variants often exhibit schizophrenia-associated behavioral abnormalities. As hypomorphic or hypermorphic NRG1 signals persists throughout life in these genetic mutants (that is, is not temporally controlled), the evaluation of these models is challenging in regard to the neurodevelopmental hypothesis.

Recently, we described the localization of ErbB4 mRNA in the midbrain dopaminergic neurons in mice and primates including humans.[20,21] Our *in situ* hybridization detected high levels of ErbB4 mRNA signals in almost all midbrain dopaminergic neurons. In particular, the expression is higher from the late embryonic stage to neonatal stage when these neurons are vigorously developing.[20,22] However, the nature of NRG1 activity on dopaminergic development or function is still poorly understood.[23]

In this study, we have designed an experimental protocol based on the neurodevelopmental hypothesis of schizophrenia[24–26] and assessed the pathological roles of excess NRG1 signals on dopaminergic neurons and their functions during and after development.[27] As upregulation of type-1 NRG1 expression is reported in schizophrenia brain pathology,[4,5] we selected this isoform of NRG1 protein and administered it to the periphery of mouse pups. The immediate and delayed impact of NRG1 treatment on developing dopaminergic neurons was analyzed using neurochemical and anatomical approaches. Furthermore, we discuss the use of NRG1-treated mice as a model for schizophrenia and compare it with other genetic mutant mice of this gene.

Materials and methods

Generation of recombinant NRG1β1 protein

A cDNA for the ectodomain (46–634 nucleotides) of mouse NRG1β1[28] was subcloned into the pET-22b (+) vector (Novagen, Madison, WI, USA) and expressed as histidine-tagged recombinant protein in *Escherichia coli* (BL21 DE3, Novagen). Inclusion bodies were denatured and solubilized by 6 M guanidine–HCl, and then NRG1β1 was purified with HiTrap Chelating HP column (GE Healthcare Bio-Science AB, Uppsala, Sweden). Denatured NRG1β1 protein was refolded by gradual removal of guanidine–HCl by means of stepwise dialysis in the presence of L-arginine and oxidized glutathione.[29] We purified a biologically active form of NRG1β1 protein with cation exchange chromatography (HiTrap-CM-FF, GE Healthcare). The peak fractions that induced ErbB4 phosphorylation in cultured neocortical neurons were used in this study (Supplementary Figure S1). The full mature form of recombinant NRG1β1 protein carries the tag sequence of six histidine residues at its carboxyl terminal end and has calculated molecular weight of 25 400 Da. Alternatively, we obtained the core epidermal growth factor domain of human NRG1β1 (eNRG1; molecular weight 7500 Da, Pepro-Tech EC, London, UK), which is an artificial product common to all NRG1 splice variants.

Animals and drug treatment

Pregnant C57BL/6NCrj mice were purchased from Nihon Charles River (Kanagawa, Japan), and their newborn pups were used in the following experiments. NRG1β1 or eNRG1 (both 1.0 $\mu g\,g^{-1}$ body weight) was administered subcutaneously daily to half of the littermates during postnatal days (PNDs) 2–10.[30] Control littermates received an injection of phosphate-buffered saline (vehicle) of the same volume. The given dose of NRG1β1 was the highest one that did not produce growth retardation in neonatal mice. A dose of NRG1β1 (3.0 $\mu g\,g^{-1}$ body weight) significantly attenuated body weight gain in the postnatal period (88.0 ± 1.3%, compared with control mice).

Risperidon (Risperdal, Janssen Pharmaceutical KK, Tokyo, Japan) was daily administered (1.0 $\mu g\,g^{-1}$) intraperitoneally on PNDs 42–70 to induce the chronic medication state of patients.[31–33] The same volume of physiological saline was administered as a control. Behavioral testing was conducted 24 h after the final antipsychotic administration to minimize sedative effects of risperidon. All the animal procedures were approved by the Animal Use and Care Committee of Niigata University and performed in accordance with the National Institute of Health (NIH) guideline (USA).

In situ *hybridization and immunohistochemistry*

Mice were anesthetized with halothane (Takeda Pharmaceutical, Osaka, Japan) and transcardially perfused with 4% paraformaldehyde. Brains were immersed in 30% sucrose and embedded in OCT compound (Sakura Finetek, Torrance, CA, USA). Coronal sections (20- to 40-μm thick) were prepared for *in situ* hybridization and immunohistochemistry. Alternatively, histopathological examination was performed by Klüver–Barrera stain (see Supplementary Materials and Methods).

For *in situ* hybridization, sections were hybridized with digoxigenin (DIG)-labeled antisense cRNA probe to ErbB4 mRNA (GenBank: NM_010154. 429–1042 nucleotides) and then with alkaline phosphatase-conjugated anti-DIG antibody as fully described previously.[20] For immunostaining, alternatively, sections were incubated with anti-c-fos (1:20000, Calbiochem, La Jolla, CA, USA) or anti-TH (1:1000, Millipore, Bedford, MA, USA) antibodies, followed by the biotinylated anti-rabbit immunoglobulin antibody (1:200, Vector Laboratories, Burlingame, CA, USA). The detection of primary antibodies or injected biotinylated NRG1β1[34] was performed with the conventional peroxidase-conjugated avidin complexes. To confirm the specificity of the avidin/biotin reaction, some of the sections were pretreated with the avidin/biotin blocking agent (Vector Laboratories). Immunoreactivity was observed using an all-in-one

microscope (BZ-9000, Keyence, Osaka, Japan) and a BZ-Analyzer (Keyence).

Immunoprecipitation and immunoblotting

For immunoprecipitation, whole brain or midbrain of mice (PND 2) was homogenized in RIPA buffer (50 mM Tris–HCl buffer pH 7.4 plus 1% Triton X-100, 1% sodium deoxycholate, 0.1% SDS, 150 mM NaCl, 5 mM EDTA, 1 mM Na_3VO_4, and 1 mM NaF) containing protease inhibitor cocktail (Complete Mini, Roche, Mannheim, Germany). Protein lysate (2 mg protein) was then incubated with the anti-ErbB4 antibody (2 μg) overnight. The antigen–antibody complex was recovered with Protein G Sepharose beads (GE Healthcare) and subjected to immunoblotting as described below.

Brain tissues were homogenized in the sample lysis buffer (62.5 mM Tris–HCl pH 6.8, 2% SDS, 0.5% NP-40, 5 mM EDTA) plus the protease inhibitor cocktail. Protein samples (5–50 μg per lane) were separated by SDS–polyacrylamide gel electrophoresis and transferred to nitrocellulose membranes. Membranes were probed with antibodies directed against phosphotyrosine (1:1000, Millipore), ErbB4 (1:1000, Santa Cruz Biotechnology, Santa Cruz, CA, USA), tyrosine hydroxylase (TH) (1:1000, Millipore), dopamine-β-hydroxylase (DBH) (1:500, Millipore), dopamine transporter (DAT) (1:1000, Millipore), vesicular monoamine transporter 2 (vMAT2) (1:1000, Millipore), D1 dopamine receptor (D1DR) (1:500, Santa Cruz Biotechnology), D2 dopamine receptor (D2DR) (1:250, Millipore), catechol-*O*-methyltransferase (COMT) (1:8000, BD Transduction Laboratories, Lexington, KY, USA), norepinephrine/noradrenaline transporter (NET) (1:500, Millipore) and β-actin (1:4000, Millipore). Alternatively, immunoblots were probed with antibodies directed against glutamatergic, GABAergic, glial markers and phospho/nonphospho-TrkB proteins (see Supplementary Materials and Methods). Immunoreactivity on membranes was detected by peroxidase-conjugated anti-immunoglobulin antibodies followed by chemiluminescence reaction combined with X-ray film exposure (ECL kit, GE Healthcare).

Behavioral testing

All behavioral tests were performed at PNDs 56–84. Spontaneous locomotor activity, acoustic startle response and prepulse inhibition (PPI) were measured as fully described previously.[35] The test paradigm of context- and tone-dependent fear learning was performed in a conditioning chamber and different test chamber (both; $10L \times 10W \times 10H$ cm box; Obaraika, Tokyo, Japan).[35,36] Freezing behavior was automatically monitored by a video camera during all sessions and analyzed by imaging software (Obaraika). The latent inhibition test was performed with the same conditioning and test chambers.[37] For auditory brainstem-evoked response testing, social interaction and further details of individual behavioral tests, see Supplementary Materials and Methods.

Methamphetamine challenge

The effects of methamphetamine (MAP) were monitored with an automated locomotor activity monitor (Med Associates, St Albans, VT, USA). Mice were placed in an activity chamber, and their horizontal activities were recorded at 5-min intervals. Mice were first habituated to the apparatus for 60 min and then challenged by MAP (Dainippon-Sumitomo Pharmaceuticals, Osaka, Japan, 1.0 or 2.0 μg g^{-1}, intraperitoneally) or saline. For quantification of c-fos-positive cells, mice were fixed as described above 2 h after a single injection of MAP. We quantified the number of c-fos-positive cells in digital microscopic images using the NIH Image cell-counting system (ver. 1.61).[38]

Surgery and microdialysis

Mice were anesthetized with pentobarbital (50 mg kg^{-1}, Somnopentyl, Schering Plough Animal Health, Kenilworth, NJ, USA) and mounted on a stereotaxic frame. Stainless guide cannula (AG-4, Eicom, Kyoto, Japan) with a dummy probe (AD-4, Eicom) was placed in the medial prefrontal cortex (mpFC, equivalent to prelimbic cortex) (coordinates: anterior +2.0 mm, lateral +0.5 mm, ventral −6.0 mm relative to the bregma). A probe was perfused with artificial cerebrospinal fluid (ACSF: 147 mM NaCl, 2.7 mM KCl, 1.2 mM $CaCl_2$, 0.5 mM $MgCl_2$) or ACSF containing high potassium (69.7 mM NaCl, 80 mM KCl, 1.2 mM $CaCl_2$, 0.5 mM $MgCl_2$) at the flow rate of 0.7 μl min^{-1}. Dialysate samples (20 μl) were collected every 30 min.

Quantification of monoamines, their metabolites and L-DOPA

The enzymatic activity of TH was assessed by monitoring the production of 3,4-dihydroxy-L-phenylalanine (L-DOPA) from tyrosine using high-performance liquid chromatography (HPLC) equipped with an electrochemical detector as fully described previously.[39] Contents of dopamine, dihydroxyphenylacetic acid (DOPAC) and homovanillic acid (HVA) and L-DOPA were determined by HPLC using a C18 column (model CA-5ODS, 4.6 × 150 mm, Eicom).[39] Dialysis samples were directly applied onto the HPLC system equipped with BDS Hypersil C18 column (1.0 × 100 mm, Keystone Scientific, Bellefonte, PA, USA). For details, see Supplementary Materials and Methods.

Statistical analysis

Statistical analyses were performed using SPSS 11.0 (SPSS Co., Tokyo, Japan). As the initial analyses of variance of behavioral data yielded no significant outcomes involving the gender variable, the data of the two genders were combined for final analyses. Fisher's least significant difference *post hoc* analysis was used to detect differences of absolute behavioral values. Alternatively, univariate data in two groups were subjected to unpaired two-tailed *t*-test. A *P*-value < 0.05 was regarded as statistically significant.

Results

Peripheral NRG1β1 crosses BBB and reaches the midbrain of mouse neonates

As the blood–brain barrier (BBB) of neonatal mice is not fully developed and may allow cytokines to penetrate into the brain,[30,40] we tested the BBB permeability of the full-length mature type-1 NRG1β1 (hereafter, referred to as NRG1β1) in mouse pups. We administered NRG1β1 (1.0 μg g^{-1}, subcutaneously) to PND 2 mice and examined the phosphorylation of NRG1 receptors (ErbB4). NRG1 administration increased the immunoreactivity for phospho-ErbB4 in the whole brain as well as in the midbrain (Figures 1a and b). The maximal activation of

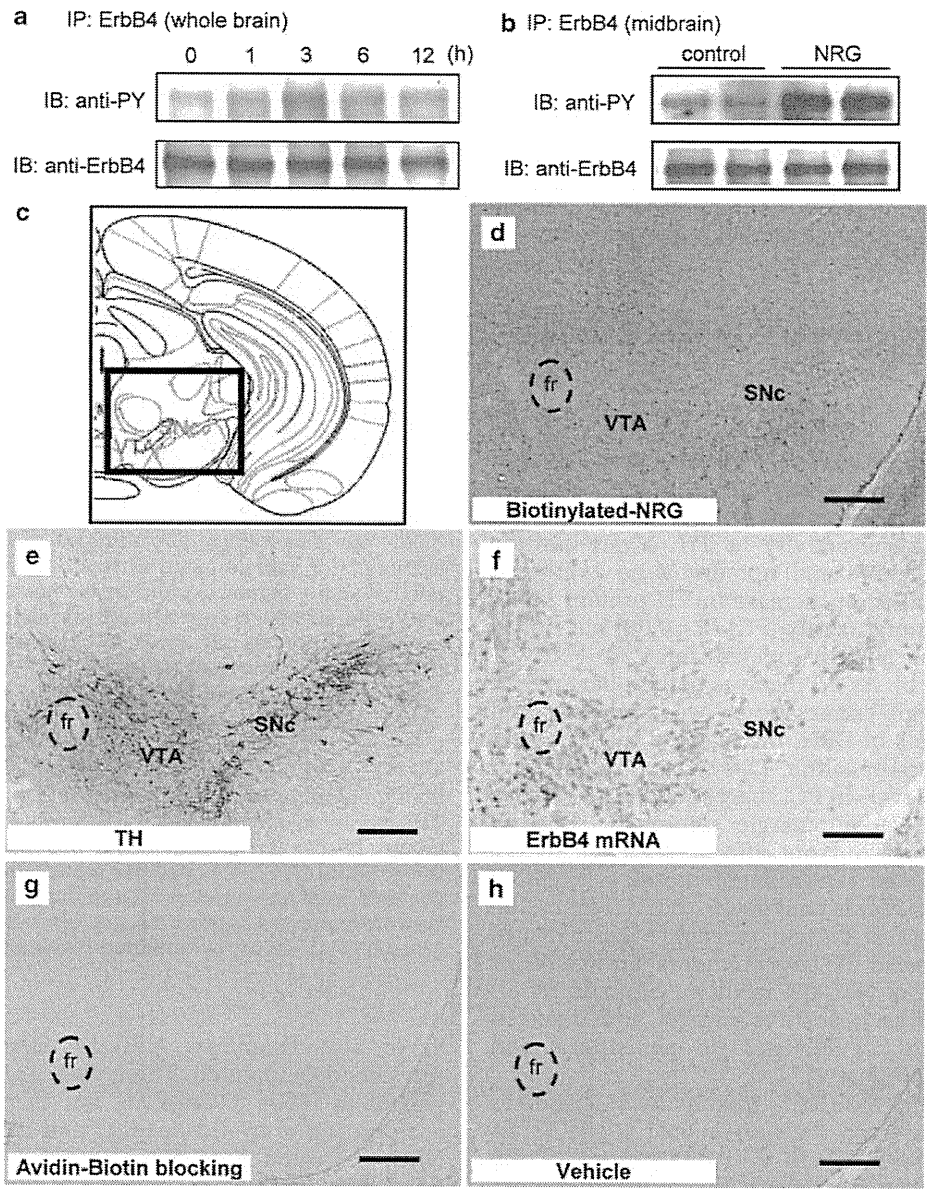

Figure 1 Penetration of administered neuregulin-1 (NRG1)β1 through the blood–brain barrier. (**a**) The whole brain lysates were prepared at 0, 1, 3, 6 and 12 h after subcutaneous injection of NRG1β1 to neonatal mice (postnatal day (PND) 2), immunoprecipitated (IP) with the anti-ErbB4 antibody and subjected to immunoblotting (IB) with anti-phosphotyrosine (anti-PY) or anti-ErbB4 antibodies. (**b**) ErbB4 phosphorylation in the midbrain was similarly examined 3 h after NRG1β1 treatment ($N = 4$ mice per group). Distributions of biotinylated NRG1β1 in the midbrain region of the enclosed area in (**c**) were examined with the avidin/biotinylated horseradish peroxidase complex. (**d**) Brain section was prepared from biotinylated-NRG1β1-injected mice. Adjoining serial sections were stained with (**e**) the anti-tyrosine hydroxylase (TH) antibody or (**f**) an *in situ* hybridization probe to ErbB4 mRNA. (**g**) Section prepared from biotinylated-NRG1β1-injected mice was pretreated with the avidin/biotin blocking reagent. (**h**) Brain section was prepared from vehicle-injected mice. fr, fasciculus retroglexus; a landmark for the midbrain; VTA, ventral tegmental area; SNc, substantia nigra pars compacta. Scale bar: 200 μm.

ErbB4 was obtained ~3 h after injection presumably because of slow penetration rates across BBB as seen with other cytokines.[30] By injecting the biotinylated form of NRG1β1, we confirmed its penetration across the neonatal BBB. Significant levels of biotin signal were detected in the intracellular space as well as on cell surfaces in the midbrain (Figure 1d), potentially representing endocytosis of the ligand-bound ErbB4 receptors.[41] This region contained TH-positive cells and ErbB4 mRNA (Figures 1e and f). Biotin signals were also detected in other brain regions (data not shown) but not when sections were pretreated with an avidin/biotin blocking agent (Figure 1g). The control sections prepared from vehicle-treated animals failed to exhibit a biotin signal (Figure1h). These results suggest that, during neonatal and possibly during perinatal stages, NRG1 circulating in the periphery can reach the midbrain and activate ErbB4 receptors of dopaminergic neurons.

Effects of neonatal NRG1β1 treatment on developing dopaminergic system

ErbB4, the receptor for NRG1, is expressed exclusively by the midbrain dopamine neurons.[20] To study the developmental effects of exogenous NRG1 on these neurons, we repeatedly administered NRG1β1 to mouse neonates (subcutaneously, PNDs 2–10). We then determined the protein expression, phosphorylation and enzyme activity of TH, a rate-limiting enzyme of dopamine and noradrenaline synthesis. We found a significant increase in TH protein levels in the whole frontal cortex (FC) ($P<0.05$) but not in the striatum of NRG1β1-treated mice at PND 11 (Figures 2a and b). As FC receives both dopaminergic and noradrenergic innervations, we also examined the protein levels of DBH, the enzyme that converts dopamine to noradrenaline. There was no significant change in DBH levels in FC, suggesting limited effects of NRG1β1 on noradrenergic neurons. Although NRG1β1 treatment did not affect TH levels in the striatum, there was a significant increase in ser-40 phosphorylation of this enzyme ($P<0.05$) (Figure 2b), a process known to elevate the enzyme activity of TH.[42] We also tested the core epidermal growth factor domain peptide of NRG1β1 (eNRG1, common for all splice variants) as a positive control and detected similar increases in TH and its phosphorylation (Supplementary Figure 2).

We found that NRG1β1 treatment in neonates significantly increased the enzyme activity of TH in the striatum and FC (both $P<0.05$) (Figure 2c). In parallel, dopamine contents in FC and the striatum were elevated in NRG1β1-treated mice at PND 11 (FC: $P<0.05$, striatum: $P<0.01$) (Figure 2d). However, there were no differences in the dopamine metabolites, DOPAC and HVA, or in noradrenaline (DOPAC: 95.7 ± 3.0%; HVA: 107.2 ± 1.9%; noradrenaline: 94.1 ± 7.1% of control). These results suggest that neonatal treatment with NRG1β1 promotes aberrant phenotypic development of midbrain dopamine neurons during neonatal and postnatal stages.

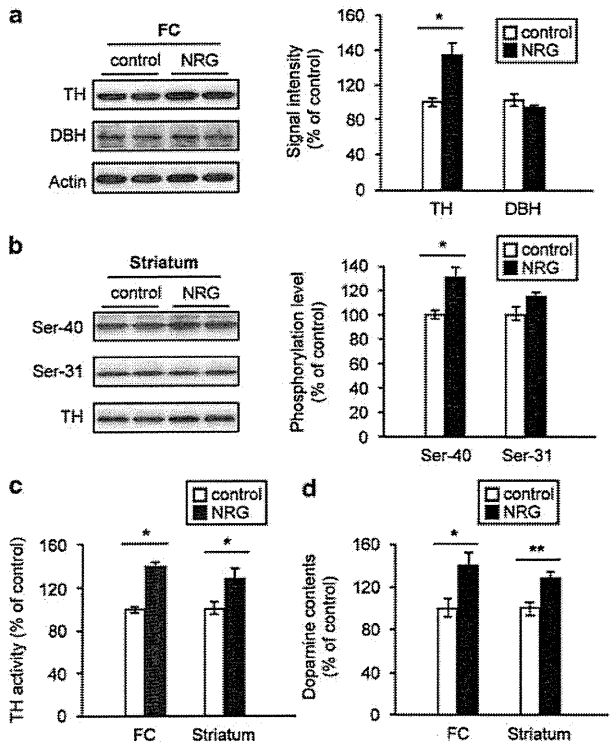

Figure 2 Effects of neonatal neuregulin-1 (NRG1)β1 treatment on developing dopaminergic neurons. NRG1β1 (1.0 μg g^{-1}) or vehicle (control) was administered (subcutaneously) daily to mouse pups during postnatal days (PNDs) 2–10, and effects on dopaminergic systems were evaluated. (**a**) Protein levels of tyrosine hydroxylase (TH) and dopamine-β-hydroxylase (DBH) in the frontal cortex (FC) were analyzed by immunoblotting and quantified by densitometric analysis, and normalized to β-actin levels ($N=6$ mice per group). (**b**) The phosphorylation (ser-40 and ser-31) levels of TH in the striatum were analyzed by immunoblotting and are presented as the ratio of phospho-TH immunoreactivity to total TH levels ($N=6$–7 mice per group). (**c**) Enzyme activity of TH was analyzed in FC and the striatum ($N=7$–11 mice per group). (**d**) The dopamine contents were measured in FC and the striatum on PND 11. Data are expressed as mean ± s.e.m ($N=7$–8 mice per group). $^*P<0.05$, $^{**}P<0.01$, by unpaired two-tailed *t*-test.

We also examined NRG1β1 effects on mouse physical development. There were no effects on body weight at PNDs 11 and 56, but there was a slight acceleration of eyelid opening and tooth eruption in NRG1β1-treated mice (Supplementary Tables S1 and S2). Thus, the transient exogenous supply of NRG1β1 seems to produce limited influences on physical indices in mouse development.

Neonatal NRG1β1 treatment induces dopaminergic hyperinnervation in adult FC

To estimate the long-term effect of neonatal NRG1β1 treatment on the dopaminergic system, we measured the levels of dopamine and its metabolites in FC, the nucleus accumbens (NAc) and striatum at the adult

stage as well (PNDs 56–70). We found significant increases in dopamine metabolites, DOPAC and HVA, in FC (DOPAC: 130.0 ± 14.0%, $P<0.05$; HVA: 131.0 ± 13.5% of control, $P<0.01$, $N=10$–12 mice per group). However, there was no significant effect on dopamine in FC (105.6 ± 6.9% of control) or on dopamine and its metabolites in the other regions (dopamine, 104.0 ± 7.7%; DOPAC, 101.1 ± 8.0; HVA, 100.1 ± 8.0% of control in NAc, $N=9$ mice per group; and dopamine, 110.8 ± 6.6%; DOPAC, 106.9 ± 8.7%; HVA, 105.5 ± 4.2% of control in the striatum, $N=10$–12 mice per group). To evaluate morphological influences, we marked the dopaminergic somata and fibers with TH immunostaining and examined them in serial coronal sections of FC and the midbrain at the adult stage. Denser or thicker axon terminals appeared to be distributed in the deep cortical layers of mpFC (i.e. prelimbic cortex) of NRG1β1-treated mice (Figures 3a–f). In contrast, there were no apparent differences in the frequency and arborization of these axons in other subregions of FC or in the midbrain (Supplementary Figure S3).

To ascertain that neonatal NRG1β1 treatment resulted in the dopaminergic hyperinnervation of

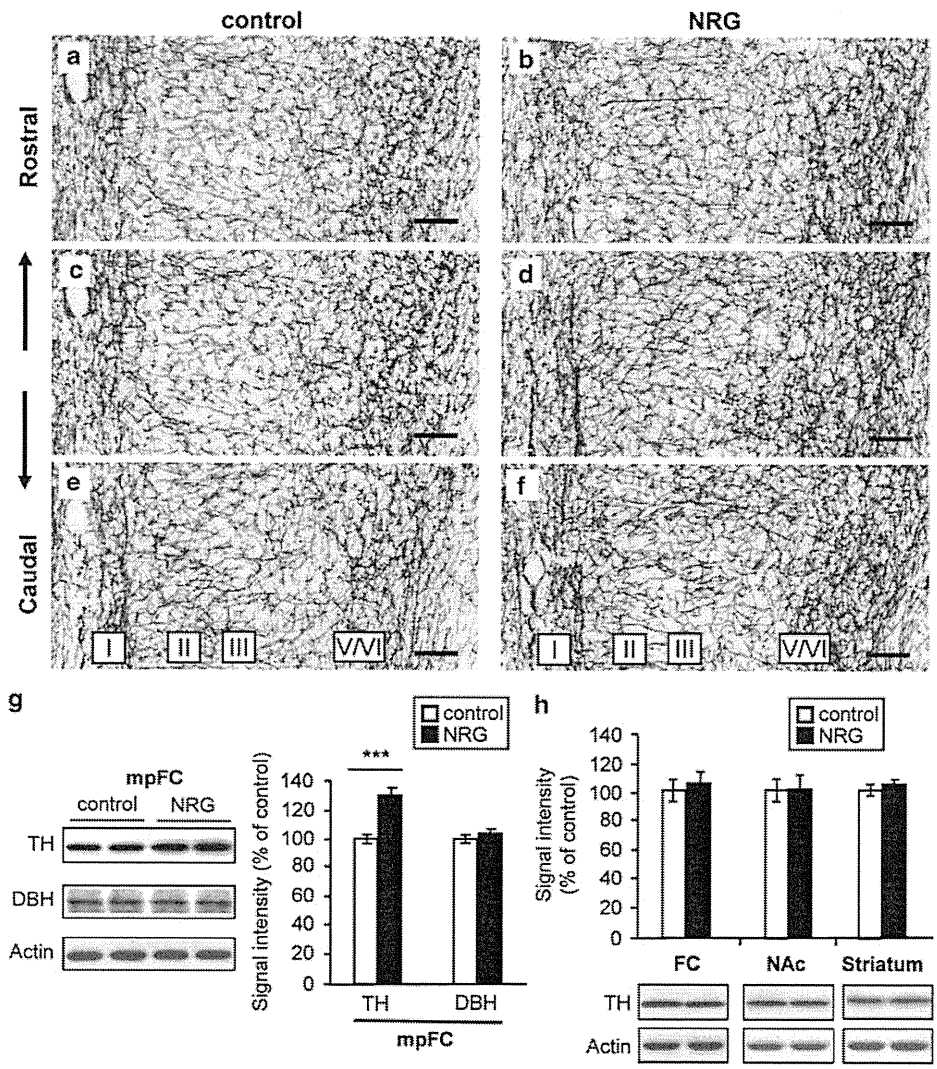

Figure 3 Neonatal exposure to neuregulin-1 (NRG1)β1 results in persistent increases in tyrosine hydroxylase (TH)-positive terminals and TH protein levels in adult medial prefrontal cortex (mpFC). Serial coronal sections of FC were prepared from vehicle-treated control and NRG1β1-treated mice and immunostained with the anti-TH antibody. TH-immunoreactive fibers in mpFC of vehicle-treated control (**a**, **c** and **e**) and NRG1β1-treated mice (**b**, **d** and **f**) are shown at the positions (**a**, **b**) +2.22 mm, (**c**, **d**) +1.98 mm and (**e**, **f**) +1.70 mm, all from the bregma. ($N=3$ mice per group). Scale bar: 100 μm. TH protein levels in mpFC, whole FC (FC), the nucleus accumbens (NAc) and striatum were measured by immunoblotting at the adult stage. (**g**) Protein levels of TH and dopamine-β-hydroxylase (DBH) in the mpFC were analyzed by immunoblotting and quantified by densitometric analysis and normalized to β-actin levels ($N=6$ mice per group). (**h**) Similarly, protein levels of TH in whole FC (FC), NAc and the striatum were analyzed ($N=5$–6 mice per group). ***$P<0.001$, by unpaired two-tailed *t*-test.

mpFC at the adult stage, we examined TH protein levels with immunoblotting. In agreement, there was a significant increase in TH protein levels in the mpFC (131.0 ± 4.3% of control, $P<0.001$) (Figure 3g). There was no change in DBH levels in the mpFC of NRG1β1-treated mice. This TH increase was not manifested by immunoblotting for the whole FC, NAc or striatum (Figure 3h).

Higher levels of dopamine release in the NRG1β1-treated mice verify their hyperdopaminergic states

The increases in dopamine metabolites and TH protein levels may lead to enhanced dopamine transmission at the adult stage. To test this hypothesis, we carried out *in vivo* microdialysis in mpFC. Although neonatal NRG1β1 treatment had no effect on the basal levels of extracellular dopamine (Figure 4a), potassium depolarization evoked higher amounts of dopamine release in mpFC of NRG1β1-treated mice (NRG1 treatment, $F_{(1,12)}=4.00$, $P<0.05$) (Figure 4b). The reason underlying failure in detecting the difference in basal dopamine release awaits further investigation. We also examined molecular markers related to dopamine transmission; DAT, vMAT2, D1DR, D2DR, COMT and NET. We did not detect significant changes in these proteins in mpFC, NAc or the striatum of NRG1β1-treated mice (Figures 4c and d).

In addition to the effects on the dopaminergic system, neonatal exposure to NRG1β1 might also influence the development of gamma-aminobutyric acid (GABA) neurons, glutamatergic synapses, glial cells or other neurotrophic signaling.[12,13,43–45] Using the conventional pathological staining as well as immunoblotting, we examined brain structures and neuronal/glial markers of NRG1β1-treated mice in the adult stage (PND 56). Klüver–Barrera staining revealed that there were no apparent structural abnormalities in adult NRG1β1-treated mice (Supplementary Figure S4). In addition, there were no significant differences in the protein levels of the glutamatergic, GABAergic and glial markers (Supplementary Figure S5), and TrkB phosphorylation (Supplementary Figure S6) between NRG1β1-treated and vehicle-treated control mice.

Neonatal NRG1β1 treatment enhances behavioral and neurochemical sensitivity to MAP

We tested whether neonatal NRG1β1 treatment alters acute responsiveness to MAP in this study. A systemic challenge of MAP (1.0 μg g^{-1}, intraperitoneally)

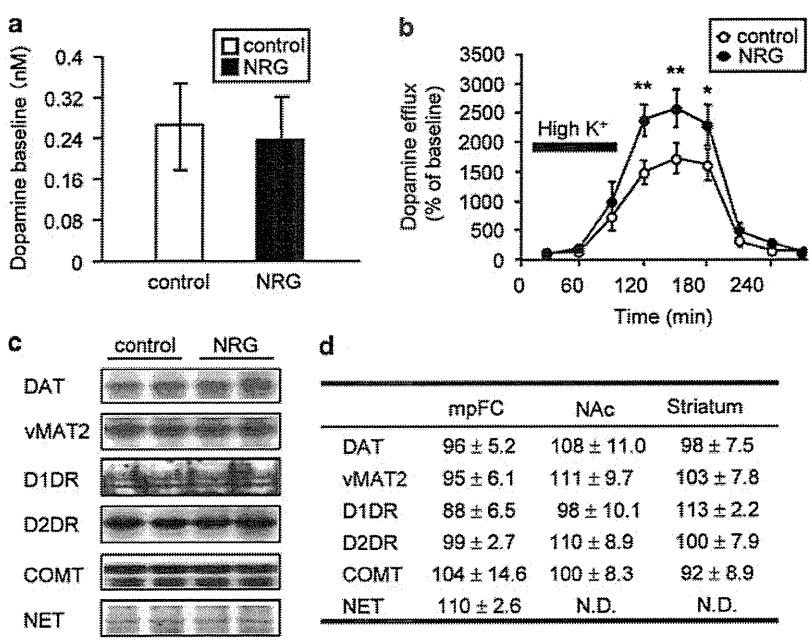

d

	mpFC	NAc	Striatum
DAT	96 ± 5.2	108 ± 11.0	98 ± 7.5
vMAT2	95 ± 6.1	111 ± 9.7	103 ± 7.8
D1DR	88 ± 6.5	98 ± 10.1	113 ± 2.2
D2DR	99 ± 2.7	110 ± 8.9	100 ± 7.9
COMT	104 ± 14.6	100 ± 8.3	92 ± 8.9
NET	110 ± 2.6	N.D.	N.D.

Figure 4 Analysis of neonatal neuregulin-1 (NRG1)β1 treatment effects on adult dopamine release and on neurochemical markers of dopaminergic neurons. Neonatal mice were treated with NRG1β1 or vehicle (control) as described in Figure 2. At the adult stage (postnatal days (PNDs) 63–70), microdialysis study was carried out in the medial prefrontal cortex (mpFC). (**a**) Basal extracellular levels of dopamine were monitored for 150 min ($N=7$ mice per group). (**b**) Dopamine release was evoked by perfusion of 80 mM KCl over 90 min (solid bar) and monitored for 270 min. Data represent relative dopamine levels in 30-min fractions (% of baseline, mean ± s.e.m, $N=7$ mice per group). $^*P<0.05$, $^{**}P<0.001$, by Fisher's least significant difference. Protein extracts were prepared at the adult stage (PNDs 56–84) from mpFC, the nucleus accumbens (NAc) and striatum of mice that were neonatally treated with NRG1β1 or vehicle (control) and subjected to immunoblotting with antibodies directed against the indicated dopaminergic markers. (**c**) Typical immunoreactive signals of two mpFC samples were displayed. (**d**) Immunoreactivities were measured by densitometric analysis and normalized to β-actin levels ($N=5$–7 mice per group). Relative levels of the protein markers in NRG1β1-treated mice are presented (% of control; mean ± s.e.m). ND, not determined. Note: There were no significant differences in all pairs.

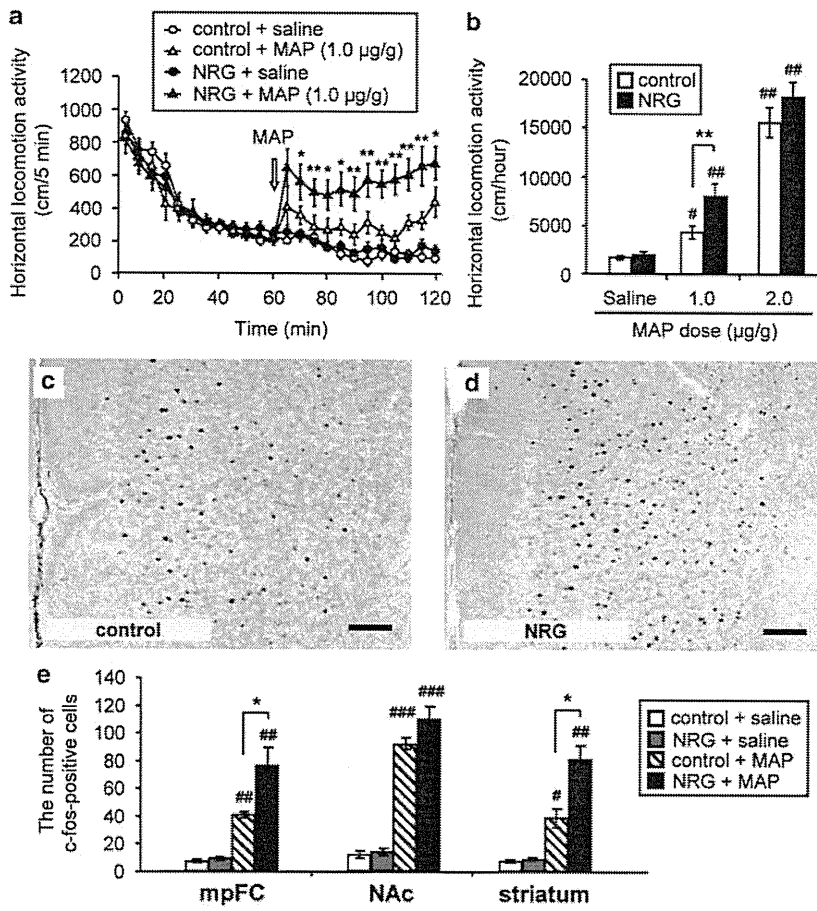

Figure 5 Neonatal exposure to neuregulin-1 (NRG1)β1 enhances locomotor activity and c-fos expression following methamphetamine (MAP) challenge. (**a**) Horizontal locomotor activity was monitored before and after MAP (1.0 μg g^{-1}) or saline challenge at the adult stage. (**b**) Total locomotor activity was calculated and presented for the 60-min period after saline or MAP (1.0 or 2.0 μg g^{-1}) challenge (N= 9–10 mice per group). (**c**) Vehicle-treated control and (**d**) NRG1β1-treated mice were subjected to c-fos immunohistochemistry 2 h after MAP (1.0 μg g^{-1}) challenge. Typical pictures of the medial prefrontal cortex (mpFC) are shown for mice challenged with MAP. Scale bar, 100 μm. (**e**) The number of c-fos-positive cells in the above microscopic field (725 × 965 μm) was counted bilaterally using the NIH Image cell-counting system (ver. 1.61) using five to seven sections of FC (+1.70 to +1.98 mm from the bregma), the nucleus accumbens (NAc) and striatum (+1.18 to +1.54 mm from the bregma), averaged for each mouse and subjected to statistical analysis (N=4 mice per group). Data are expressed as mean ± s.e.m. $^{*}P<0.05$, $^{**}P<0.01$, compared between marked groups. $^{\#}P<0.05$, $^{\#\#}P<0.01$, $^{\#\#\#}P<0.001$, compared between MAP-challenged and -unchallenged groups by Fisher's least significant difference.

increased locomotor activity in both NRG1β1-treated and control groups (MAP, $F_{(1,36)}=16.30$, $P<0.001$). However, the magnitude of MAP-induced locomotor activity was significantly higher in NRG1β1-treated group than the control group (NRG1 treatment, $F_{(1,36)}=5.14$, $P<0.05$; NRG1 treatment × MAP, $F_{(1,36)}=4.34$, $P<0.05$) (Figure 5a). The acceleration of MAP sensitivity by neonatal NRG1β1 treatment seemed to depend on the MAP dose (MAP dose, $F_{(1,54)}=162$, $P<0.001$). At a dose of 2.0 μg g^{-1} of MAP, the effect of NRG1β1 treatment became less apparent ($P=0.052$) (Figure 5b). Thus, these results indicate that mice neonatally exposed to NRG1β1 exhibited higher sensitivity to the lower dose of MAP.

We also examined c-fos expression in the brain following MAP challenge (1.0 μg g^{-1}) (Figure 5e). We found that MAP challenge induced a greater number of c-fos-positive cells in mpFC and the striatum in NRG1β1-treated mice than in control mice (both $P<0.01$) (Figures 5c–e). In contrast, there were no significant effects of NRG1β1 treatment in NAc (Figure 5e).

Neonatal NRG1β1 treatment impairs sensorimotor gating at the adult stage

We assessed sensorimotor gating of NRG1β1-treated mice by measuring PPI, which is often implicated in schizophrenia pathology or dopaminergic

dysfunction.[46,47] We found a significant reduction of PPI in the NRG1β1-treated group (NRG1 treatment, $F_{(1,22)}=6.91$, $P<0.05$) (Figure 6a) with no significant effect on pulse-alone startle (Figure 6b). As NRG1 signaling is involved in the survival of cochlear sensory neurons,[48] we also tested hearing ability by measuring auditory brainstem-evoked response thresholds. There were no differences in the auditory stimulus thresholds at any frequency between the two groups (Figure 6c).

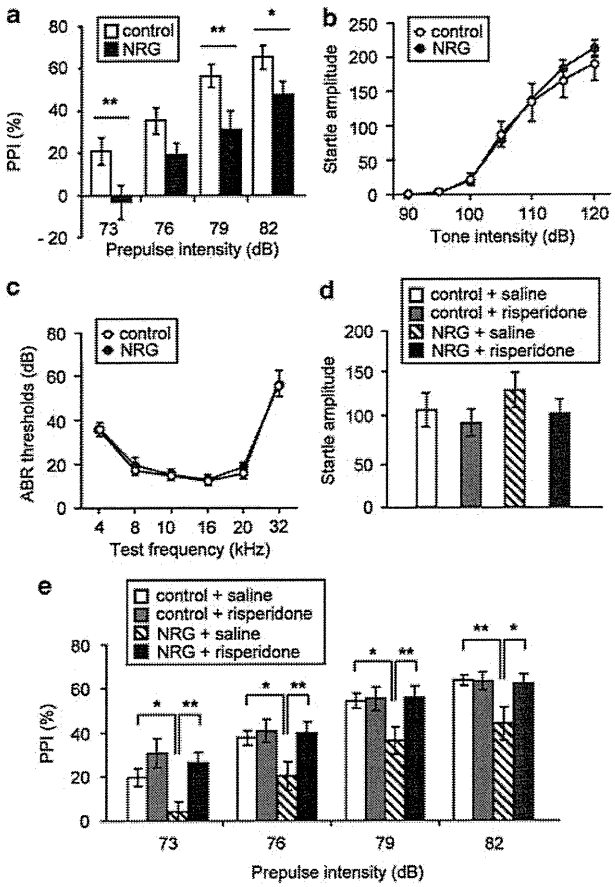

Figure 6 Effects of neonatal exposure to neuregulin-1 (NRG1)β1 on hearing, startle responses and PPI. Neonatal mice were treated with NRG1β1 or vehicle (control) as described in Figure 2. At the adult stage, PPI levels, acoustic startle responses and brainstem-evoked response (ABR) thresholds were determined. (**a**) PPI was measured with 73, 76, 79 and 82 dB prepulse stimuli ($N=12$ mice per group). (**b**) Relative amplitudes of startle responses were monitored with 90, 95, 100, 105, 110, 115 and 120 dB tones ($N=10$ mice per group). (**c**) ABR thresholds were examined with specific auditory stimuli (4, 8, 10, 16, 20 and 32 kHz) by varying the sound pressure levels ($N=9$–10 mice per group). Pharmacological responses of NRG1β1-treated mice to risperidone were examined by PPI measurement. Mice daily received risperidone (1.0 μg g^{-1}, intraperitoneally) or saline during postnatal days (PNDs) 42–70. On 1 day after final administration of risperidone, PPI test was performed. (**d**) Effects of risperidone on pulse-alone startle (120 dB) were presented ($N=10$ mice per group). (**e**) Amelioration of PPI deficits in NRG1β1-treated mice by risperidone ($N=10$ mice per group). Data are expressed as mean ± s.e.m. $^*P<0.05$, $^{**}P<0.01$, by Fisher's least significant difference.

Risperidone, an atypical antipsychotic, has been shown to reduce psychotic symptoms and ameliorate PPI deficits in schizophrenia patients and in the animal models of schizophrenia.[49] Using a chronic administration schedule, we investigated the effect of risperidone (1.0 μg g^{-1}, daily) on PPI deficits in NRG1β1-treated mice. Risperidone administration significantly improved PPI deficits of NRG1β1-treated mice compared with control mice (drug, $F_{(1,36)}=7.46$, $P<0.01$) (Figure 6e). However, it did not significantly alter the amplitudes of pulse-alone startle (Figure 6d).

Neonatal NRG1β1 treatment alters latent inhibition and social behaviors

We assessed the basal locomotor activity of adult mice, which influences behavioral evaluation of learning. There was no significant difference in locomotor activity scores between NRG1β1-treated and vehicle-treated control mice (NRG1 treatment, $F_{(1,23)}=1.17$, $P=0.29$) (Supplementary Figure S7a). Then learning ability of these mice was measured with context- and tone-dependent fear conditioning. We found that NRG1β1 treatment in neonates did not alter learning performance in either paradigm (NRG1 treatment, $F_{(1,20)}=0.41$, $P=0.53$ for the context-dependent learning; $F_{(1,20)}=0.21$, $P=0.66$ for the tone-dependent learning) (Supplementary Figure S7b).

As NRG1β1-treated mice exhibited normal locomotion and fear learning, the mice were subjected to latent inhibition test. Latent inhibition of learning is considered to be an ability to ignore irrelevant stimuli and has been shown to involve the dopaminergic system.[50,51] This process is often disrupted in schizophrenia patients.[52] Although basal learning scores were indistinguishable in non-pre-exposure (NPE) groups, the inhibitory effect of pre-exposure (PE) on freezing scores was different between vehicle-treated and NRG1β1-treated groups (NRG1 treatment × pre-exposure, $F_{(1,48)}=4.23$, $P<0.05$) (Figures 7a and b). In contrast to the significant latent inhibition of vehicle-treated mice ($P<0.01$), there was no significant difference in freezing rates between the NPE and PE groups of NRG1β1-treated mice ($P=0.78$) (Figure 7c), indicating their lack of latent inhibition.

To investigate the impact of neonatal NRG1β1 treatment on adult social behaviors in adulthood, we used a resident-intruder behavioral assay. In this assay, a group-housed male mouse (intruder) was placed in another home cage where a resident mouse had been housed alone until the test day. We found that male NRG1β1-treated mice (residents) showed a significant decrease in the duration and frequency of social interactions compared with vehicle-treated control male residents (both $P<0.01$) (Figures 7d and e). On the other hand, the duration of fighting behavior was indistinguishable between NRG1β1- and vehicle-treated control mice (Figure 7f).

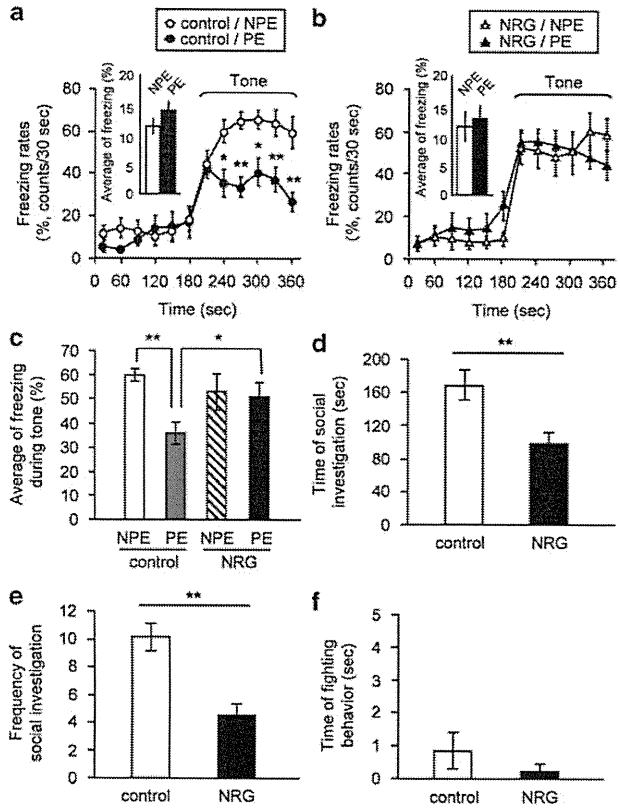

Figure 7 Mice neonatally exposed to neuregulin-1 (NRG1)β1 show impaired latent inhibition and reduced social interaction. NRG1β1-treated and vehicle-treated mice were pre-exposed to tone cue (PE group) or not exposed to the cue (non-pre-exposure (NPE) group) and then subjected to tone-footshock pairs. On 1 day after conditioning, freezing rates (%) of (**a**) vehicle-treated control and (**b**) NRG1β1-treated mice were measured every 30 s in a different chamber before and during tone exposure. Insets reveal mean freezing rates during conditioning ($N=12$–14 mice per group). (**c**) Mean freezing rates during tone exposure in test trial. Social interaction was evaluated by the resident-intruder assay. We measured (**d**) time spent by the resident males over 10-min period actively pursing social investigation of the intruder mouse, (**e**) frequency of social behavior and (**f**) total time duration of fighting behavior ($N=7$–8 mice per group). Data are expressed as mean ± s.e.m. $^{*}P<0.05$, $^{**}P<0.01$, by Fisher's least significant difference.

Discussion

In support of the neurodevelopmental hypothesis for the etiology of schizophrenia, here, we found the neuropathological implication of abnormal signals of the risk gene, *NRG1*. Specifically, we showed the profound influences of transient hyper-NRG1 signals on developing midbrain dopaminergic systems, evaluating the subacute and delayed neurochemical and behavioral consequences. Exogenous administration of NRG1β1 protein to mouse neonates produced the activation of midbrain ErbB4 receptors and caused marked changes in dopaminergic neurons and their associated behaviors: (1) Neonatal treatment of NRG1β1 increased the protein levels, phosphorylation, enzyme activity of TH and elevated dopamine levels in FC and/or the striatum; (2) In adulthood, NRG1β1-treated mice exhibited sustained increases in dopamine metabolism and depolarization-triggered dopamine release in FC; (3) NRG1β1-treated mice were more sensitive to MAP in regard to locomotor activity and c-fos induction; (4) NRG1β1-treated mice showed behavioral abnormalities in PPI, social interactions and latent inhibition. These results reveal a novel neurotrophic activity of NRG1 on developing midbrain dopaminergic neurons *in vivo* and indicate a biological link between prenatal or perinatal NRG1 and the dopaminergic pathology of schizophrenia. In contrast to the abnormalities in the dopaminergic systems described above, our examinations failed to uncover any gross structural deficits and neuronal or glial abnormalities with conventional dye staining and immunostatining. In addition, learning ability and basal locomotor activity were preserved in this animal model.

Influences of NRG1β1 on brain structure and function

Neuregulin-1 has a variety of neurotrophic activities on neuronal migration, axon guidance, myelination and synaptogenesis.[12–15] We assessed the influences of NRG1β1 on these neurotrophic processes in this model by quantifying the following neuronal and glial phenotypic markers in various brain regions: neuron-specific enolase, glial fibrillary acidic protein, myelin basic protein, 2′,3′-cyclic nucleotide 3′-phosphodiesterase, glutamate and GABA receptors (GluR1, GluR2/3, NMDAR1, NMDAR2A/B, GABAARα1), glutamate decarboxylase 65/67 and parvalbumin. However, there were no apparent neurochemical alterations in any of these molecular markers.

In contrast to these results, previous studies on knockout and transgenic mice of *NRG1* or *ErbB* genes show that abnormal NRG1 signals result in phenotypic alterations such as impairments in myelin formation, migration of GABAergic interneurons and glial development.[12,13,44,45] We assume that the absence of phenotypic influences in our model could be due to (1) saturation of neurotrophic supports for these cells by other factors, (2) the distinct developmental time window of individual cell types or (3) difference in biological activities of individual NRG1 splicing variants.

Gene targeting in mice shows that the development of neuronal and glial cells are supported by multiple neurotrophic factors and cytokines.[53] Thus, signal redundancy by multiple neurotrophic factors can help explain the phenotypic differences seen between this NRG1β1 model and the genetic mutant models described earlier. Exogenously supplied NRG1 may not have pronounced effects on GABAergic neurons and glial cells if the same or similar factors endogenously provide a saturated level of neurotrophic support for these cells. Conversely,

midbrain dopaminergic neurons might not receive enough neurotrophic support from endogenous NRG1 and be therefore competent to fully react to exogeneous NRG1 in this model. In this context, it is noteworthy that ErbB4 knockout mice did not exhibit any significant structural or neurochemical alterations in midbrain dopaminergic neurons.[54]

In this study, we limited the exposure period of NRG1β1 to PNDs 2–10, which matches the developmental period of midbrain dopaminergic neurons.[55,56] In this context, it is possible that this cell population is relatively sensitive to NRG1β1 and dynamically reacts with this factor during the used experimental period. Thus, if we changed the timing of the NRG1β1 administration, the effect or affected cell population would differ.

Another possible explanation is based on the difference in biological activities of NRG1 splicing variants (types 1–5).[57–59] Type-1 and type-2 NRG1 proteins comprise the extracellular Ig-like domain that interacts with heparan sulfate proteoglycans and modifies receptor binding and signaling.[60] In contrast, type-3 NRG1 has an activity to regulate oligodendrocyte development and myelination.[13] The specific use of type-1 NRG1β1 in the present experiments might therefore limit its biological effects.

Neurotrophic activity of NRG1 on midbrain dopaminergic neurons

In this study, we found subacute effects of neonatal NRG1β1 treatment on developing dopaminergic systems. Interestingly, the influence of neonatal treatment with NRG1β1 was persistent in mpFC until adulthood. In adult mice treated with NRG1β1 as neonates, there were elevated dopaminergic innervation and metabolism. These results indicate that neonatal exposure to NRG1β1 can lead to lifelong impairment of dopamine synthesis and release in this brain region.

Dopaminergic innervation in the brain is classified into the three fiber routes: mesostriatal, mesolimbic and mesofrontocortical pathways. As ErbB4 mRNA is distributed in almost all classes of midbrain dopaminergic neurons in mice and primates,[20,21] these results raised a question regarding pathway specificity of the long-term effects of NRG1β1 treatment: Why was a dopaminergic abnormality persistent and apparent in mpFC? We would like to elaborate on the differences in developmental schedules among three dopaminergic pathways as follows.

In regard to the temporal schedule of development, there is significant time lag in the development of mesostriatal, mesolimbic and mesofrontocortical dopamine pathways. In rodents, the dopaminergic projections to the striatum and NAc are more extensive during midgestation.[55] In contrast, dopaminergic projections to the neocortical and limbic regions is vigorous at postnatal stages.[56,61] Thus, our hypothesis is that, at the postnatal stage when NRG1β1 was administered, corticolimbic fibers were still growing and capable of responding to this neurotrophic factor.

Behavioral similarity to genetic mutant mice

By targeting individual exons in the *NRG1* gene, various types of knockout mice for *NRG1* gene were developed, and their behavioral deficits were extensively investigated and compared.[1,16,17,19] There are some similarities in behavioral traits between NRG1β1-administered mice in this study and NRG1 knockout mice in published reports, even though these models presumably use an opposite strategy of NRG1 to reduce NRG1 signals. For example CRD-NRG1$^{+/-}$ mice exhibited PPI deficits and Ig-NRG1$^{+/-}$ mice have abnormalities in latent inhibition as seen in the present NRG1-injection model.[16,19] In this context, there is an interesting report that transgenic mice overexpressing type-1 NRG1 exhibited similar behavioral deficits in PPI.[62]

Different types of NRG1 precursors, which are produced from a single gene, carry the distinct transmembrane domain(s) and are subjected to different modes of proteolytic regulation (for example, ectodomain shedding).[57] We established this animal model by stimulating ErbB receptors with processed type-1 NRG1 in a paracrine manner. This counter-intuitive similarity between this model and these knockout mice might be explained by determining how individual exon disruption influences juxtacrine and paracrine/autocrine signaling of the remaining NRG1 variants and how it affects the molecular interaction of individual NRG1 variants with distinct ErbB receptors.[12,13,15,16,63] Future studies should elucidate the biological characteristics of individual NRG1 variants and their precursors as well as their compensation or interference.[57–59]

NRG1β1-treated mice as an animal model for schizophrenia

Schizophrenia patients show increased sensitivity to various dopamine agonists or releasers, such as amphetamine and cocaine.[64] Local or systemic administration of dopamine agonists to animals elicits the behavioral deficits in PPI as well as latent inhibition and social interactions that are implicated in schizophrenia,[46,51,65] suggesting pathological contribution of hyperdopaminergic states to this disease.[66] In this study, neonatal NRG1β1 treatment resulted in similar behavioral deficits as well as persistent dopaminergic impairments in adulthood. *In vivo* microdialysis and monoamine measurement verified the hyperdopaminergic state of NRG1β1-treated mice. This argument is also supported by the hypersensitivity of this model to MAP. Furthermore, chronic treatment of risperidone ameliorated the deficits in PPI in NRG1β1-treated mice. Chronic antipsychotic treatment selectively decreases dopamine transmission in FC,[67] although different brain regions are also involved in PPI abnormality.[68] Although a plenty of controversies and discrepancies against the roles of dopamine in schizophrenia remain, our findings with the NRG1β1-treated mice provide evidence in favor of a hyperdopaminergic state in schizophrenia, at least within FC.[68–70]

In contrast, the pathological link between the dopaminergic abnormality and the social deficits of this mouse model is controversial, as the reduction in social interaction is rather ascribed to the hypodopaminegic or serotonergic deficits.[27,71] In this context, we do not exclude the possibility that uncovered neurochemical deficits of NRG1β1-treated mice still remains to be explored.

Pathological implication of NRG1β1 in neurodevelopmental hypothesis of schizophrenia

The SNPs of the *NRG1* gene that associate with the risk for schizophrenia are often located in the promoter region of *NRG1* gene[1] and presumably involved in positive regulation of *NRG1* gene transcription.[5] In agreement, post-mortem studies support the association of increased NRG1 mRNA or protein with schizophrenia.[3–5] Depending on the SNP type of *NRG1*, ischemic and traumatic brain injury may induce higher levels of NRG1 expression.[10,11] In this context, NRG1 is one of the candidate molecules that might be involved in both genetic and environmental vulnerabilities to schizophrenia.[72]

Maternal infections and fetal/neonatal hypoxia are potential environmental risk factors for schizophrenia and are used in its animal modeling.[7,8,73] Interestingly, the animal models established by the immune inflammatory insults also exhibit impaired dopaminergic innervations or metabolism.[74–76] In this context, it is noteworthy that NRG1 is highly inducible in fetuses and neonates in response to these environmental insults.[9,10] Therefore, it is possible that NRG1 and potentially other ErbB4 ligands might contribute to the dopaminergic impairment of these animal models as well as that of schizophrenia.[25,26]

On the basis of the neurodevelopmental hypothesis,[24–26] we have tested various inflammatory cytokines and neurotrophic factors to address the question of whether they can mediate the environmental insults for schizophrenia risk.[77] Among many factors examined, neonatal treatment only with epidermal growth factor, interleukin-1 and NRG1 produce the long-lasting behavioral impairments that are implicated in schizophrenia models.[40,66,78] Interestingly, these factors have a common neurotrophic activity on midbrain dopaminergic neurons.[30,40] However, we did not detect any neurobehavioral influences of control proteins (cytochrome c and albumin) in the *in vivo* experimental paradigm.[40,77,78]

In conclusion, NRG1 is one of the key neurotrophic factors that have crucial impact on dopaminergic development and its neuropathology. We hope that this model established with NRG1 will facilitate the validation of both neurodevelopmental and dopaminergic hypotheses of schizophrenia.

Conflict of interest

HN was a recipient of the research grants from Astrazeneca Pharmaceutical Inc.

Acknowledgments

We are grateful to Dr Jourdi for proofreading. This work was supported by Health and Labor Sciences Research Grants, a grant for Promotion of Niigata University Research Projects, Core Research for Evolutional Science and Technology from the JST Corporation and a grant-in-aid from the Ministry of Health, Labor and Welfare, Japan.

Note added in proof: We also tested the *in vivo* activity of the misfolded NRG1β1 in the peak 1 of the cation-exchange chromatography (Supplementary Figure S1) and did not detect its effects on TH and dopamine content (Supplementary Figure S8).

References

1 Stefansson H, Sigurdsson E, Steinthorsdottir V, Bjornsdottir S, Sigmundsson T, Ghosh S *et al.* Neuregulin 1 and susceptibility to schizophrenia. *Am J Hum Genet* 2002; **71**: 877–892.
2 Walsh T, McClellan JM, McCarthy SE, Addington AM, Pierce SB, Cooper GM *et al.* Rare structural variants disrupt multiple genes in neurodevelopmental pathways in schizophrenia. *Science* 2008; **320**: 539–543.
3 Chong VZ, Thompson M, Beltaifa S, Webster MJ, Law AJ, Weickert CS. Elevated neuregulin-1 and ErbB4 protein in the prefrontal cortex of schizophrenic patients. *Schizophr Res* 2008; **100**: 270–280.
4 Hashimoto R, Straub RE, Weickert CS, Hyde TM, Kleinman JE, Weinberger DR. Expression analysis of neuregulin-1 in the dorsolateral prefrontal cortex in schizophrenia. *Mol Psychiatry* 2004; **9**: 299–307.
5 Law AJ, Lipska BK, Weickert CS, Hyde TM, Straub RE, Hashimoto R *et al.* Neuregulin 1 transcripts are differentially expressed in schizophrenia and regulated by 5′ SNPs associated with the disease. *Proc Natl Acad Sci USA* 2006; **103**: 6747–6752.
6 Petryshen TL, Middleton FA, Kirby A, Aldinger KA, Purcell S, Tahl AR *et al.* Support for involvement of neuregulin 1 in schizophrenia pathophysiology. *Mol Psychiatry* 2005; **10**: 366–374.
7 Brown AS, Begg MD, Gravenstein S, Schaefer CA, Wyatt RJ, Bresnahan M *et al.* Serologic evidence of prenatal influenza in the etiology of schizophrenia. *Arch Gen Psychiatry* 2004; **61**: 774–780.
8 Zornberg GL, Buka SL, Tsuang MT. Hypoxic-ischemia-related fetal/neonatal complications and risk of schizophrenia and other nonaffective psychoses: a 19-year longitudinal study. *Am J Psychiatry* 2000; **157**: 196–202.
9 Nadri C, Belmaker RH, Agam G. Oxygen restriction of neonate rats elevates neuregulin-1alpha isoform levels: possible relationship to schizophrenia. *Neurochem Int* 2007; **51**: 447–450.
10 Parker MW, Chen Y, Hallenbeck JM, Ford BD. Neuregulin expression after focal stroke in the rat. *Neurosci Lett* 2002; **334**: 169–172.
11 Tokita Y, Keino H, Matsui F, Aono S, Ishiguro H, Higashiyama S *et al.* Regulation of neuregulin expression in the injured rat brain and cultured astrocytes. *J Neurosci* 2001; **21**: 1257–1264.
12 Flames N, Long JE, Garratt AN, Fischer TM, Gassmann M, Birchmeier C *et al.* Short- and long-range attraction of cortical GABAergic interneurons by neuregulin-1. *Neuron* 2004; **44**: 251–261.
13 Taveggia C, Thaker P, Petrylak A, Caporaso GL, Toews A, Falls DL *et al.* Type III neuregulin-1 promotes oligodendrocyte myelination. *Glia* 2008; **56**: 284–293.
14 Krivosheya D, Tapia L, Levinson JN, Huang K, Kang Y, Hines R *et al.* ErbB4-neuregulin signaling modulates synapse development and dendritic arborization through distinct mechanisms. *J Biol Chem* 2008; **283**: 32944–32956.
15 López-Bendito G, Cautinat A, Sánchez JA, Bielle F, Flames N, Garratt AN *et al.* Tangential neuronal migration controls axon

guidance: a role for neuregulin-1 in thalamocortical axon navigation. *Cell* 2006; **125**: 127–142.
16 Chen YJ, Johnson MA, Lieberman MD, Goodchild RE, Schobel S, Lewandowski N *et al.* Type III neuregulin-1 is required for normal sensorimotor gating, memory-related behaviors, and corticostriatal circuit components. *J Neurosci* 2008; **28**: 6872–6883.
17 Ehrlichman RS, Luminais SN, White SL, Rudnick ND, Ma N, Dow HC *et al.* Neuregulin 1 transgenic mice display reduced mismatch negativity, contextual fear conditioning and social interactions. *Brain Res* 2009; **1294**: 116–127.
18 O'Tuathaigh CM, Babovic D, O'Sullivan GJ, Clifford JJ, Tighe O, Croke DT *et al.* Phenotypic characterization of spatial cognition and social behavior in mice with 'knockout' of the schizophrenia risk gene neuregulin 1. *Neuroscience* 2007; **147**: 18–27.
19 Rimer M, Barrett DW, Maldonado MA, Vock VM, Gonzalez-Lima F. Neuregulin-1 immunoglobulin-like domain mutant mice: clozapine sensitivity and impaired latent inhibition. *Neuroreport* 2005; **16**: 271–275.
20 Abe Y, Namba H, Zheng Y, Nawa H. *In situ* hybridization reveals developmental regulation of ErbB1-4 mRNA expression in mouse midbrain: implication of ErbB receptors for dopaminergic neurons. *Neuroscience* 2009; **161**: 95–110.
21 Zheng Y, Watakabe A, Takada M, Kakita A, Namba H, Takahashi H *et al.* Expression of ErbB4 in substantia nigra dopamine neurons of monkeys and humans. *Prog Neuropsychopharmacol Biol Psychiatry* 2009; **33**: 701–706.
22 Fox IJ, Kornblum HI. Developmental profile of ErbB receptors in murine central nervous system: implications for functional interactions. *J Neurosci Res* 2005; **79**: 584–597.
23 Neddens J, Vullhorst D, Paredes D, Buonanno A. Neuregulin links dopaminergic and glutamatergic neurotransmission to control hippocampal synaptic plasticity. *Commun Integr Biol* 2009; **2**: 261–264.
24 Lewis DA, Levitt P. Schizophrenia as a disorder of neurodevelopment. *Annu Rev Neurosci* 2002; **25**: 409–432.
25 Murray RM, Lewis SW. Is schizophrenia a neurodevelopmental disorder? *Br Med J* 1987; **295**: 681–682.
26 Weinberger DR. Implications of normal brain development for the pathogenesis of schizophrenia. *Arch Gen Psychiatry* 1987; **44**: 660–669.
27 Winterer G, Weinberger DR. Genes, dopamine and cortical signal-to-noise ratio in schizophrenia. *Trends Neurosci* 2004; **27**: 683–690.
28 Ozaki M, Tohyama K, Kishida H, Buonanno A, Yano R, Hashikawa T. Roles of neuregulin in synaptogenesis between mossy fibers and cerebellar granule cells. *J Neurosci Res* 2000; **59**: 612–623.
29 Umetsu M, Tsumoto K, Hara M, Ashish K, Goda S, Adschiri T *et al.* How additives influence the refolding of immunoglobulin-folded proteins in a stepwise dialysis system. Spectroscopic evidence for highly efficient refolding of a single-chain Fv fragment. *J Biol Chem* 2003; **278**: 8979–8987.
30 Tohmi M, Tsuda N, Zheng Y, Mizuno M, Sotoyama H, Shibuya M *et al.* The cellular and behavioral consequences of interleukin-1 alpha penetration through the blood-brain barrier of neonatal rats: a critical period for efficacy. *Neuroscience* 2007; **150**: 234–250.
31 Kapur S, VanderSpek SC, Brownlee BA, Nobrega JN. Antipsychotic dosing in preclinical models is often unrepresentative of the clinical condition: a suggested solution based on *in vivo* occupancy. *J Pharmacol Exp Ther* 2003; **305**: 625–631.
32 Lim EP, Verma V, Nagarajah R, Dawe GS. Propranolol blocks chronic risperidone treatment-induced enhancement of spatial working memory performance of rats in a delayed matching-to-place water maze task. *Psychopharmacology (Berl)* 2007; **191**: 297–310.
33 Martinez-Gras I, Rubio G, del Manzano BA, Rodriguez-Jimenez R, Garcia-Sanchez F, Bagney A *et al.* The relationship between prepulse inhibition and general psychopathology in patients with schizophrenia treated with long-acting risperidone. *Schizophr Res* 2009; **115**: 215–221.
34 Namba H, Zheng Y, Abe Y, Nawa H. Epidermal growth factor administered in the periphery influences excitatory synaptic inputs onto midbrain dopaminergic neurons in postnatal mice. *Neuroscience* 2009; **158**: 1731–1741.
35 Tohmi M, Tsuda N, Mizuno M, Takei N, Frankland PW, Nawa H. Distinct influences of neonatal epidermal growth factor challenge on adult neurobehavioral traits in four mouse strains. *Behav Genet* 2005; **35**: 615–629.
36 Frankland PW, Josselyn SA, Anagnostaras SG, Kogan JH, Takahashi E, Silva AJ. Consolidation of CS and US representations in associative fear conditioning. *Hippocampus* 2004; **14**: 557–569.
37 Caldarone BJ, Duman CH, Picciotto MR. Fear conditioning and latent inhibition in mice lacking the high affinity subclass of nicotinic acetylcholine receptors in the brain. *Neuropharmacology* 2000; **39**: 2779–2784.
38 Brown HE, Garcia MM, Harlan RE. A two focal plane method for digital quantification of nuclear immunoreactivity in large brain areas using NIH-image software. *Brain Res Brain Protoc* 1998; **2**: 264–272.
39 Mizuno M, Sotoyama H, Narita E, Kawamura H, Namba H, Zheng Y *et al.* A cyclooxygenase-2 inhibitor ameliorates behavioral impairments induced by striatal administration of epidermal growth factor. *J Neurosci* 2007; **27**: 10116–10127.
40 Futamura T, Kakita A, Tohmi M, Sotoyama H, Takahashi H, Nawa H. Neonatal perturbation of neurotrophic signaling results in abnormal sensorimotor gating and social interaction in adults: implication for epidermal growth factor in cognitive development. *Mol Psychiatry* 2003; **8**: 19–29.
41 Liu Y, Tao YM, Woo RS, Xiong WC, Mei L. Stimulated ErbB4 internalization is necessary for neuregulin signaling in neurons. *Biochem Biophys Res Commun* 2007; **354**: 505–510.
42 Fujisawa H, Okuno S. Regulatory mechanism of tyrosine hydroxylase activity. *Biochem Biophys Res Commun* 2005; **338**: 271–276.
43 Ozaki M, Sasner M, Yano R, Lu HS, Buonanno A. Neuregulin-beta induces expression of an NMDA-receptor subunit. *Nature* 1997; **390**: 691–694.
44 Sardi SP, Murtie J, Koirala S, Patten BA, Corfas G. Presenilin-dependent ErbB4 nuclear signaling regulates the timing of astrogenesis in the developing brain. *Cell* 2006; **127**: 185–197.
45 Roy K, Murtie JC, El-Khodor BF, Edgar N, Sardi SP, Hooks BM *et al.* Loss of erbB signaling in oligodendrocytes alters myelin and dopaminergic function, a potential mechanism for neuropsychiatric disorders. *Proc Natl Acad Sci USA* 2007; **104**: 8131–8136.
46 Broersen LM, Feldon J, Weiner I. Dissociative effects of apomorphine infusions into the medial prefrontal cortex of rats on latent inhibition, prepulse inhibition and amphetamine-induced locomotion. *Neuroscience* 1999; **94**: 39–46.
47 Grillon C, Ameli R, Charney DS, Krystal J, Braff D. Startle gating deficits occur across prepulse intensities in schizophrenic patients. *Biol Psychiatry* 1992; **32**: 939–943.
48 Stankovic K, Rio C, Xia A, Sugawara M, Adams JC, Liberman MC *et al.* Survival of adult spiral ganglion neurons requires erbB receptor signaling in the inner ear. *J Neurosci* 2004; **24**: 8651–8661.
49 Kumari V, Soni W, Sharma T. Prepulse inhibition of the startle response in risperidone-treated patients: comparison with typical antipsychotics. *Schizophr Res* 2002; **55**: 139–146.
50 Gray NS, Pickering AD, Hemsley DR, Dawling S, Gray JA. Abolition of latent inhibition by a single 5 mg dose of d-amphetamine in man. *Psychopharmacology (Berl)* 1992; **107**: 425–430.
51 Peleg-Raibstein D, Knuesel I, Feldon J. Amphetamine sensitization in rats as an animal model of schizophrenia. *Behav Brain Res* 2008; **191**: 190–201.
52 Baruch I, Hemsley DR, Gray JA. Differential performance of acute and chronic schizophrenics in a latent inhibition task. *J Nerv Ment Dis* 1998; **176**: 598–606.
53 Nawa H, Takahashi M, Patterson PH. Cytokine and growth factor involvement in schizophrenia-support for the developmental model. *Mol Psychiatry* 2000; **5**: 594–603.
54 Thuret S, Alavian KN, Gassmann M, Lloyd CK, Smits SM, Smidt MP *et al.* The neuregulin receptor, ErbB4, is not required for normal development and adult maintenance of the substantia nigra pars compacta. *J Neurochem* 2004; **91**: 1302–1311.
55 Hu Z, Cooper M, Crockett DP, Zhou R. Differentiation of the midbrain dopaminergic pathways during mouse development. *J Comp Neurol* 2004; **476**: 301–311.

56 Kalsbeek A, Voorn P, Buijs RM, Pool CW, Uylings HB. Development of the dopaminergic innervation in the prefrontal cortex of the rat. *J Comp Neurol* 1998; **269**: 58–72.
57 Falls FL. Neuregulins: functions, forms, and signaling strategies. *Exp Cell Res* 2003; **284**: 14–30.
58 Harrison PJ, Law AJ. Neuregulin 1 and schizophrenia: genetics, gene expression, and neurobiology. *Biol Psychiatry* 2006; **60**: 132–140.
59 Mei L, Xiong WC. Neuregulin 1 in neural development, synaptic plasticity and schizophrenia. *Nat Rev Neurosci* 2008; **9**: 437–452.
60 Li Q, Loeb JA. Neuregulin-heparan-sulfate proteoglycan interactions produce sustained erbB receptor activation required for the induction of acetylcholine receptors in muscle. *J Biol Chem* 2001; **276**: 38068–38075.
61 Brummelte S, Teuchert-Noodt G. Postnatal development of dopamine innervation in the amygdala and the entorhinal cortex of the gerbil (Meriones unguiculatus). *Brain Res* 2006; **1125**: 9–16.
62 Deakin IH, Law AJ, Oliver PL, Schwab MH, Nave KA, Harrison PJ *et al*. Behavioural characterization of neuregulin 1 type I overexpressing transgenic mice. *Neuroreport* 2009; **20**: 1523–1528.
63 Canoll PD, Musacchio JM, Hardy R, Reynolds R, Marchionni MA, Salzer JL. GGF/neuregulin is a neuronal signal that promotes the proliferation and survival and inhibits the differentiation of oligodendrocyte progenitors. *Neuron* 1996; **17**: 229–243.
64 Lieberman JA, Kane JM, Alvir J. Provocative tests with psychostimulant drugs in schizophrenia. *Psychopharmacology (Berl)* 1987; **91**: 415–433.
65 Clemens KJ, Van Nieuwenhuyzen PS, Li KM, Cornish JL, Hunt GE, McGregor IS. MDMA ('ecstasy'), methamphetamine and their combination: long-term changes in social interaction and neurochemistry in the rat. *Psychopharmacology (Berl)* 2004; **173**: 318–325.
66 Lipska BK, Weinberger DR. To model a psychiatric disorder in animals: schizophrenia as a reality test. *Neuropsychopharmacology* 2000; **23**: 223–239.
67 Hernandez L, Hoebel BG. Chronic clozapine selectively decreases prefrontal cortex dopamine as shown by simultaneous cortical, accumbens, and striatal microdialysis in freely moving rats. *Pharmacol Biochem Behav* 1995; **52**: 581–589.
68 Geyer MA, Krebs-Thomson K, Braff DL, Swerdlow NR. Pharmacological studies of prepulse inhibition models of sensorimotor gating deficits in schizophrenia: a decade in review. *Psychopharmacology* 2001; **156**: 117–154.
69 Keith VA, Mansbach RS, Geyer MA. Failure of haloperidol to block the effects of phencyclidine and dizocilpine on prepulse inhibition of startle. *Biol Psychiatry* 1991; **30**: 557–566.
70 Le Pen G, Moreau JL. Disruption of prepulse inhibition of startle reflex in a neurodevelopmental model of schizophrenia: reversal by clozapine, olanzapine and risperidone but not by haloperidol. *Neuropsychopharmacology* 2002; **27**: 1–11.
71 Tamminga CA. The neurobiology of cognition in schizophrenia. *J Clin Psychiatry* 2006; **67**(Suppl 9): 9–13.
72 Jaaro-Peled H, Hayashi-Takagi A, Seshadri S, Kamiya A, Brandon NJ, Sawa A. Neurodevelopmental mechanisms of schizophrenia: understanding disturbed postnatal brain maturation through neuregulin-1-ErbB4 and DISC1. *Trends Neurosci* 2009; **32**: 485–495.
73 Shi L, Fatemi SH, Sidwell RW, Patterson PH. Maternal influenza infection causes marked behavioral and pharmacological changes in the offspring. *J Neurosci* 2003; **23**: 297–302.
74 Decker MJ, Hue GE, Caudle WM, Miller GW, Keating GL, Rye DB. Episodic neonatal hypoxia evokes executive dysfunction and regionally specific alterations in markers of dopamine signalling. *Neuroscience* 2003; **117**: 417–425.
75 Meyer U, Feldon J. Prenatal exposure to infection: a primary mechanism for abnormal dopaminergic development in schizophrenia. *Psychopharmacology (Berl)* 2009; **206**: 587–602.
76 Romero E, Guaza C, Castellano B, Borrell J. Ontogeny of sensorimotor gating and immune impairment induced by prenatal immune challenge in rats: implications for the etiopathology of schizophrenia. *Mol Psychiatry* 2008; e-pub ahead of print 15 April 2008; doi:10.1038/mp.2008.44.
77 Nawa H, Takei N. Recent progress in animal modeling of immune inflammatory processes in schizophrenia: implication of specific cytokines. *Neurosci Res* 2006; **56**: 2–13.
78 Tohmi M, Tsuda N, Watanabe Y, Kakita A, Nawa H. Perinatal inflammatory cytokine challenge results in distinct neurobehavioral alterations in rats: implication in psychiatric disorders of developmental origin. *Neurosci Res* 2004; **50**: 67–75.

Supplementary Information accompanies the paper on the Molecular Psychiatry website (http://www.nature.com/mp)